

Scalable and consistent embedding of probability measures into Hilbert spaces via measure quantization

Erell Gachon¹, Jérémie Bigot¹, and Elsa Cazelles²

¹Institut de Mathématiques de Bordeaux, Université de Bordeaux, CNRS (UMR 5251)

²CNRS, IRIT (UMR 5505), Université de Toulouse

February 10, 2025

Abstract

This paper is focused on statistical learning from data that come as probability measures. In this setting, popular approaches consist in embedding such data into a Hilbert space with either *Linearized Optimal Transport* or *Kernel Mean Embedding*. However, the cost of computing such embeddings prohibits their direct use in large-scale settings. We study two methods based on measure quantization for approximating input probability measures with discrete measures of small-support size. The first one is based on optimal quantization of each input measure, while the second one relies on mean-measure quantization. We study the consistency of such approximations, and its implication for scalable embeddings of probability measures into a Hilbert space at a low computational cost. We finally illustrate our findings with various numerical experiments.

1 Introduction

Machine Learning (ML) problems modeling data as a set of N probability measures are classical in numerous applied fields such as signal and image processing, computer vision or computational biology, see the surveys [24, 26, 32, 34]. In particular, this framework includes distribution regression [5, 6, 31, 37, 42] that consists in predicting a scalar or label response from predictors that are probability measures, and the problem of Principal Component Analysis (PCA) of a set of probability measures [8, 10, 41, 45] for the purpose of dimension reduction from so-called distributional data [3]. Performing standard ML tasks on a set of probability measures is not straightforward as the algorithms are usually designed to handle N points from an Euclidean space rather than N distributions. However, as most of these methods rely on correlations through an inner-product, a popular approach is to embed such distributional data into a Hilbert space in which the whole machinery of machine learning methods can be easily applied. The two most commonly used embeddings are as follows: the first one is based on Linearized Optimal

Transport (LOT) [14, 33, 45] and arises from the field of *Optimal Transport* (OT) [36, 40], by leveraging the Riemannian-like geometry of the space of probability measures endowed with the Wasserstein distance [2]. The second one, known as *Kernel Mean Embedding* (KME) [34], relies on the use of kernel methods to map probability measures into a *Reproducing Kernel Hilbert Space* (RKHS).

However, the computational cost and the storing of such embeddings prevent their use in large-scale settings. This is often the case when observing N empirical measures on point clouds $X^{(i)} = (X_1^{(i)}, \dots, X_{m_i}^{(i)}) \in (\mathbb{R}^d)^{m_i}, 1 \leq i \leq N$, with a large number m_i of observations. Such datasets are frequently found in flow cytometry [30], where observations collected from N patients represent a considerable amount of cells, each characterized by d bio-markers. For these single-cell data, one usually encounters point clouds of thousands to millions of events (that is $m_i \geq 10^5$) living in a feature space of dimension d larger than 10. Using either the LOT embedding or the KME from such raw data becomes critical as these approaches suffer from high computational costs as soon as the number m_i of points per clouds is larger than a few thousands.

Therefore, a relevant question is the following: given a set of N probability measures with large support size, how to efficiently compute an embedding into a Hilbert space that is statistically consistent with the embedding derived directly from the raw data ?

1.1 Main contributions

In this paper, we consider the problem of embedding a set of d -dimensional input probability measures $(\mu^{(i)})_{i=1}^N$ into a Hilbert space at a low computational cost. To that end, we propose to employ a preliminary K -quantization step that is either based on optimal quantization of each input measure $\mu^{(i)}$ or on the quantization of the mean measure $\bar{\mu} = \frac{1}{N} \sum_{i=1}^N \mu^{(i)}$ as used in [16] for single-cell data analysis. The aim of this K -quantization step is to approximate $(\mu^{(i)})_{i=1}^N$ by discrete measures $(\nu_K^{(i)})_{i=1}^N$ with supports of size K , with K typically small. Using the theory of measure quantization [19, 35], we validate both quantization approaches by showing (Prop. 3.4):

$$\mathcal{W}_2^2 \left(\frac{1}{N} \sum_{i=1}^N \delta_{\mu^{(i)}}, \frac{1}{N} \sum_{i=1}^N \delta_{\nu_K^{(i)}} \right) = O(K^{-2/d}), \quad (1)$$

where \mathcal{W}_2 denotes the 2-Wasserstein distance (4) on $\mathcal{P}(\mathcal{P}(\mathcal{X}))$, the set of probability measures over $\mathcal{P}(\mathcal{X})$, which is itself the set of probability measures with support included in a compact set $\mathcal{X} \subset \mathbb{R}^d$.

The asymptotic result (1) allows to show the convergence of numerous statistics computed from the $\nu_K^{(i)}$'s to corresponding quantities for the $\mu^{(i)}$'s as $K \rightarrow +\infty$. These statistics include the Wasserstein barycenter and the Gram matrix of the pairwise inner-products of the measures embedded to a Hilbert space using either LOT or KME. The latter is a standard quantity used in machine learning tasks (e.g. PCA).

Finally, the soundness and consistency of our method is illustrated with numerical experiments on synthetic and real datasets. We also show that the method based on

mean-measure quantization has computational advantages over optimal quantization of each input measure while preserving satisfactory performances, which justifies its use in large scale settings.

1.2 Related works

In [12, 39], quantization is employed to embed a set of N probability measures into a finite-dimensional Euclidean space through measure vectorization. More precisely, given N input measures $\mu^{(i)}$, a quantization of the mean measure $\bar{\mu} = \frac{1}{N} \sum_{i=1}^N \mu^{(i)}$ by K centers x_1, \dots, x_K in \mathbb{R}^d is first done. Then, they map each measure $\mu^{(i)}$ to $v^{(i)} = (v_1^{(i)}, \dots, v_K^{(i)})$ a vector of the convex space \mathbb{R}_+^K , where $v_k^{(i)}$ roughly represents the mass spread from the measure $\mu^{(i)}$ around the center x_k . Yet, this embedding does not take into account the relative positions of the K centers, and consistency in the sense (1) is not shown as we propose in this paper by endowing the set of quantized measures $\nu_K^{(i)}$ with the Wasserstein distance (3).

In [11], the authors tackle the problem of computing the KME of a probability distribution μ for which m samples X_1, \dots, X_m are available. They introduce an estimator of the KME of μ based on Nyström approximation that can be computed efficiently using a small random subset from the data. Their theoretical and empirical results show that this approach yields a consistent estimator of the maximum mean discrepancy distance between the KMEs of μ and $\hat{\mu}_m = \frac{1}{m} \sum_{j=1}^m \delta_{X_j}$ at a low computational cost. However, this Nyström approximation has not been studied for constructing a consistent LOT embedding estimator.

Finally, the benefits of a preliminary quantization step have been studied in [7] to improve the standard estimator of the OT cost between two probability measures based on the plug-in of their empirical counterpart. Still, the simultaneous quantization of N probability measures for the purpose of constructing consistent and scalable embeddings has not been considered so far.

1.3 Organization of the paper

Section 2 presents OT, the embeddings LOT and KME and the quantization principle. In Section 3, we describe our two quantization methods of a set of N probability measures, and analyze their theoretical properties. Section 4 reports the results of numerical experiments using synthetic and real data, and compare the computational cost of both methods. The paper ends with a conclusion in Section 5. All proofs are deferred to two technical Appendices A and B, and additional numerical experiments are given in Appendix C.

2 Background

Optimal transport. Let ρ and μ be two probability measures with support included in a compact set $\mathcal{X} \subset \mathbb{R}^d$. For the quadratic cost, the OT problem between ρ and μ is:

$$\min_{\pi \in \Pi(\rho, \mu)} \int_{\mathcal{X} \times \mathcal{X}} \|x - y\|^2 d\pi(x, y), \quad (2)$$

where $\Pi(\rho, \mu)$ is the set of probability measures (or transport plans) on $\mathcal{X} \times \mathcal{X}$ with marginals ρ and μ . For π^* a minimizer of (2), the Wasserstein metric between ρ and μ is

$$W_2(\rho, \mu) = \left(\int_{\mathcal{X} \times \mathcal{X}} \|x - y\|^2 d\pi^*(x, y) \right)^{1/2}. \quad (3)$$

Now, we endow the set of probability measures $\mathcal{P}(\mathcal{X})$ with the 2-Wasserstein distance W_2 . In this paper, we shall represent the set $(\mu^{(i)})_{1 \leq i \leq N}$ as the discrete empirical probability measure $\mathbb{P}^N = \frac{1}{N} \sum_{i=1}^N \delta_{\mu^{(i)}}$ over $\mathcal{P}(\mathcal{X})$. To define a metric on $\mathcal{P}(\mathcal{P}(\mathcal{X}))$, the set of Borel probability measures over $\mathcal{P}(\mathcal{X})$, we will use W_2^2 as the ground cost on the metric space $(\mathcal{P}(\mathcal{X}), W_2)$. The 2-Wasserstein distance over $\mathcal{P}(\mathcal{P}(\mathcal{X}))$ is then defined as [27]

$$\mathcal{W}_2(\mathbb{P}, \mathbb{Q}) = \left(\min_{\gamma \in \Gamma(\mathbb{P}, \mathbb{Q})} \int_{\mathcal{P}(\mathcal{X}) \times \mathcal{P}(\mathcal{X})} W_2^2(\rho, \mu) d\gamma(\rho, \mu) \right)^{1/2}, \quad (4)$$

where $\Gamma(\mathbb{P}, \mathbb{Q})$ is the set of probability distributions on $\mathcal{P}(\mathcal{X}) \times \mathcal{P}(\mathcal{X})$ with respective marginals \mathbb{P} and \mathbb{Q} .

LOT and KME embeddings. Given an absolutely continuous (a.c.) measure ρ , we first recall that Brenier's theorem [9] states that the optimal transport plan π^* in (2) is supported on the graph of a ρ -a.s. unique push-forward map¹ $T_\rho^\mu : \mathcal{X} \rightarrow \mathbb{R}^d$. In other words, $\pi^* = (\text{id}, T_\rho^\mu)_\# \rho$ and

$$W_2^2(\rho, \mu) = \int_{\mathcal{X}} \|x - T_\rho^\mu(x)\|^2 d\rho(x). \quad (5)$$

The LOT embedding then consists in mapping a probability measure μ into the tangent space $\mathcal{T}_\rho = \{T_\rho^\mu - \text{id}\}_{\mu \in \mathcal{P}(\mathcal{X})}$ at ρ , that is a subspace of the Hilbert space $L^2(\rho, \mathbb{R}^d) = \{v : \mathbb{R}^d \rightarrow \mathbb{R}^d \mid \int_{\mathbb{R}^d} \|v\|^2 d\rho < \infty\}$, endowed with the weighted L^2 inner product $\langle v_1, v_2 \rangle_{L^2(\rho)} = \int_{\mathbb{R}^d} v_1(x)^T v_2(x) d\rho(x)$.

Now, given a positive definite kernel function $k : \mathcal{X} \times \mathcal{X} \rightarrow \mathbb{R}$ and associated RKHS \mathcal{H} , the KME of $\mu \in \mathcal{P}(\mathcal{X})$ is the embedding $\phi : \mathcal{P}(\mathcal{X}) \rightarrow \mathcal{H}$ defined by $\phi(\mu) = \int_{\mathcal{X}} k(x, \cdot) d\mu(x)$. When the kernel k is characteristic [34], the map ϕ is injective and one can define a metric on $\mathcal{P}(\mathcal{X})$ called *Maximum Mean Discrepancy* $\text{MMD}(\rho, \mu) = \|\phi(\rho) - \phi(\mu)\|_{\mathcal{H}}$.

¹We recall that the pushforward operator of a measure ρ in \mathbb{R}^d is defined as the measure $T_\# \rho$ such that for all Borelian $B \subset \mathbb{R}^d$, $T_\# \rho = \rho(T^{-1}(B))$.

Optimal quantization. We conclude this section with reminders on the theory of quantization [19, 35]. A K -points quantization of an arbitrary probability measure μ aims at approximating μ by solving [19][Lemma 3.4]:

$$\min_{a \in \Sigma_K, X \in (\mathbb{R}^d)^K} W_2^2 \left(\mu, \sum_{k=1}^K a_k \delta_{x_k} \right), \quad (6)$$

where Σ_K is the probability simplex in \mathbb{R}^K .

Remark 2.1. If μ is a.c., it follows from [28][Proposition 2] that minimizers of (6) over $X \in (\mathbb{R}^d)^K$ exist and belong to the set of pairwise distinct points

$$F_K = \{X = (x_1, \dots, x_K) \in (\mathbb{R}^d)^K \mid x_k \neq x_\ell, \text{ if } k \neq \ell\}.$$

Given $X \in F_K$, it is well-known, see e.g. [18, 25], that the minimizer a^* of $\min_{a \in \Sigma_K} W_2^2 \left(\mu, \sum_{k=1}^K a_k \delta_{x_k} \right)$ is unique, and verifies $a_k^* = \mu(V_{x_k})$ where $(V_{x_k})_{k=1}^K$ is the set of Voronoï cells induced by X :

$$V_{x_k} = \{y \in \mathbb{R}^d \mid \forall \ell \neq k, \|x_k - y\|^2 \leq \|x_\ell - y\|^2\}. \quad (7)$$

Thereby, the quantization problem (6) rewrites as:

$$\min_{X \in (\mathbb{R}^d)^K} W_2^2 \left(\mu, \sum_{k=1}^K \mu(V_{x_k}) \delta_{x_k} \right). \quad (8)$$

Remark 2.2. If the measure μ is discrete, then the closed form solution in variable a of the quantization problem (6) remains valid provided that the definition (7) of the Voronoï cells is slightly modified as follows

$$\tilde{V}_{x_1} := V_{x_1} \quad \text{and} \quad \tilde{V}_{x_k} := V_{x_k} \setminus \bigcup_{j < k} \tilde{V}_{x_j} \quad \text{for } k \geq 2, \quad (9)$$

so that $(\tilde{V}_{x_k})_{k=1}^K$ form a partition of \mathbb{R}^d [19][Chapter 1] for $X = (x_1, \dots, x_K) \in F_K$. Then, for such a partitioning, it follows from Lemma A.1 in Appendix A that

$$\min_{a \in \Sigma_K} W_2^2 \left(\mu, \sum_{k=1}^K a_k \delta_{x_k} \right) = W_2^2 \left(\mu, \sum_{k=1}^K \mu(\tilde{V}_{x_k}) \delta_{x_k} \right) = \int_{\mathbb{R}^d} \min_{1 \leq k \leq K} \{\|x_k - y\|^2\} d\mu(y),$$

for any probability measure μ . As a consequence, and unless otherwise stated, the results of the paper hold for discrete probability measures with the choice (9) as a Voronoï partition, which corresponds to a chosen enumeration order of the elements of the set X . However, when μ is a discrete measure, it is necessary to require the cardinality of its support to be larger than K so that the minimizers of (6) belong to F_K [28][Proposition 2], and the sets of the Voronoï partition (9) are pairwise distinct.

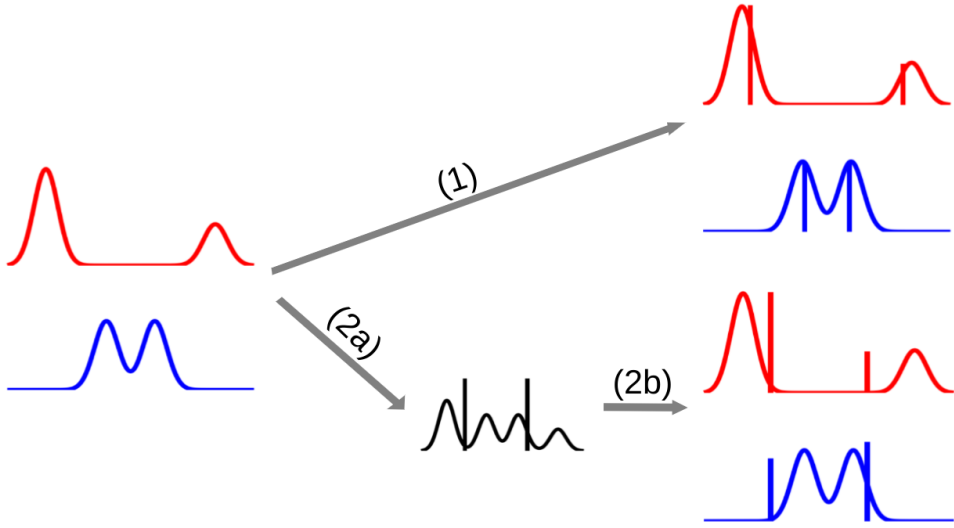


Figure 1: Illustration of the quantization methods on two 1D probability measures (left) with $K = 2$. (1) Quantization of each measure. (2a) Quantization of the mean measure. (2b) Computation of the weights for each measure. The vertical lines are located on the Dirac positions and weights of the quantized measures.

Given a K -points quantization, that is a minimizer $X^* \in (\mathbb{R}^d)^K$ of (6), the *quantization error* of the probability measure μ is defined as

$$\varepsilon_K(\mu) = \int_{\mathbb{R}^d} \min_{1 \leq k \leq K} \{\|x_k^* - y\|^2\} d\mu(y). \quad (10)$$

Theorem 6.2 in [19] then implies that $\varepsilon_K(\mu) = O(K^{-2/d})$ if μ is a.c. and $\varepsilon_K(\mu) = o(K^{-2/d})$ if μ is discrete.

3 Statistical properties of probability measures embeddings via measure quantization

Throughout this section, the supports of the probability measures $(\mu^{(i)})_{i=1}^N$ are included in a compact set $\mathcal{X} \subset \mathbb{R}^d$. To reduce the computational costs of solving ML problems involving N measures $(\mu^{(i)})_{i=1}^N$ with large supports, we propose two quantization methods, illustrated in Figure 1, to approximate the $\mu^{(i)}$'s with discrete measures supported on K points.

Optimal quantization of each input measure. A first natural approach is to approximate each $\mu^{(i)}$ by its optimal quantization

$$\tilde{\nu}_K^{(i)} = \sum_{k=1}^K \tilde{a}_k^{(i)} \delta_{x_k^{(i)}}, \quad (11)$$

where the weights $\tilde{a}^{(i)} = (\tilde{a}_k^{(i)})_{1 \leq k \leq K}$ and locations $X^{(i)} = (x_k^{(i)})_{1 \leq k \leq K}$ are minimizers of (6) for $\mu = \mu^{(i)}$.

Mean-measure quantization Our second quantization method consists in solving the following problem:

$$\min_{a \in (\Sigma_K)^N, X \in F_K} \frac{1}{N} \sum_{i=1}^N W_2^2 \left(\sum_{k=1}^K a_k^{(i)} \delta_{x_k}, \mu^{(i)} \right), \quad (12)$$

as introduced in [16] for a.c. probability distributions. The following result shows that optimizing (12) is equivalent to K -points quantization of the mean measure.

Proposition 3.1. *Let $(\mu^{(i)})_{1 \leq i \leq N}$ be arbitrary probability measures and let $\bar{\mu} = \frac{1}{N} \sum_{i=1}^N \mu^{(i)}$ be the mean measure. Suppose that the cardinality of the support of $\bar{\mu}$ is larger than K . Then,*

$$\begin{aligned} \min_{a \in (\Sigma_K)^N, X \in F_K} \frac{1}{N} \sum_{i=1}^N W_2^2 \left(\sum_{k=1}^K a_k^{(i)} \delta_{x_k}, \mu^{(i)} \right) &= \min_{X \in (\mathbb{R}^d)^N} \frac{1}{N} \sum_{i=1}^N W_2^2 \left(\sum_{k=1}^K \mu^{(i)}(\tilde{V}_{x_k}) \delta_{x_k}, \mu^{(i)} \right) \\ &= \min_{X \in (\mathbb{R}^d)^N} W_2^2 \left(\sum_{k=1}^K \bar{\mu}(\tilde{V}_{x_k}) \delta_{x_k}, \bar{\mu} \right) \end{aligned} \quad (13)$$

For a minimizer $\bar{X} = (\bar{x}_1, \dots, \bar{x}_K)$ of (13), that is a K -point quantization of $\bar{\mu}$, we then define the quantized measures for $1 \leq i \leq N$ by

$$\bar{\nu}_K^{(i)} = \sum_{k=1}^K \bar{a}_k^{(i)} \delta_{\bar{x}_k}, \text{ with } \bar{a}_k^{(i)} = \mu^{(i)}(\tilde{V}_{\bar{x}_k}), \quad (14)$$

where $(\tilde{V}_{\bar{x}_k})_{1 \leq k \leq K}$ is the Voronoï partition (9) associated to \bar{X} . The measure $\bar{\nu}_K^{(i)}$ is therefore a discrete probability measure supported on K points that is an approximation of $\mu^{(i)}$ in the sense of the minimization problem (12). The measures $(\bar{\nu}_K^{(i)})_{1 \leq i \leq N}$ differ in their weights but share the same support \bar{X} . In a slight abuse of language, we will refer to $\bar{\nu}_K^{(i)}$ as a *quantized* version of $\mu^{(i)}$, even though it is not the optimal quantization $\tilde{\nu}_K^{(i)}$ of $\mu^{(i)}$ given in (11).

Remark 3.2 (On the compactness assumption of \mathcal{X}). Proposition 3.1 remains true without the compactness of \mathcal{X} , under the assumption of 2-order moments of the measures.

Remark 3.3 (On the nature of input probability measures). (i) If all the measures $(\mu^{(i)})_{1 \leq i \leq N}$ are a.c. then $\bar{\mu}$ is also a.c. and by convention the cardinality of its support is $+\infty$. In this case, for all $i \in \{1, \dots, N\}$ and $k \in \{1, \dots, K\}$,

$$\bar{a}_k^{(i)} = \mu^{(i)}(\tilde{V}_{\bar{x}_k}) = \mu^{(i)}(V_{\bar{x}_k}),$$

as the boundaries of the Voronoï cells $(V_{\bar{x}_k})_{1 \leq k \leq K}$ have zero-mass for the Lebesgue measure.

(ii) If all the measures $(\mu^{(i)})_{1 \leq i \leq N}$ are discrete, then the definition (14) of the probability measure $(\bar{\nu}_K^{(i)})_{1 \leq i \leq N}$ is specific to the chosen Voronoï partition (9) associated to an enumeration of \bar{X} . In this setting, a minimizer \bar{a} of (12) is not necessarily unique, and another enumeration order of \bar{X} may lead to a slightly different set of quantized measures, depending on the intersection between the points clouds and the boundaries of the Voronoï cells.

For clarity, we write the Voronoï cells associated to a K -quantization \bar{X} of the mean measure $\bar{\mu}$ in Prop.3.1 as

$$V_k := \tilde{V}_{\bar{x}_k}, \quad \text{for all } 1 \leq k \leq K. \quad (15)$$

3.1 Consistency of measures quantization

The following result shows the consistency of both quantization methods by leveraging the quantization error function $\varepsilon_K(\cdot)$ defined in (10).

Proposition 3.4. *Let $\mathbb{P}^N = \frac{1}{N} \sum_{i=1}^N \delta_{\mu^{(i)}}$, $\bar{\mathbb{P}}_K^N = \frac{1}{N} \sum_{i=1}^N \delta_{\bar{\nu}_K^{(i)}}$ and $\tilde{\mathbb{P}}_K^N = \frac{1}{N} \sum_{i=1}^N \delta_{\tilde{\nu}_K^{(i)}}$. Then,*

$$\mathcal{W}_2^2(\bar{\mathbb{P}}_K^N, \mathbb{P}^N) = \frac{1}{N} \sum_{i=1}^N W_2^2(\mu^{(i)}, \bar{\nu}_K^{(i)}) = \varepsilon_K(\bar{\mu}) \quad (16)$$

and

$$\mathcal{W}_2^2(\tilde{\mathbb{P}}_K^N, \mathbb{P}^N) = \frac{1}{N} \sum_{i=1}^N W_2^2(\mu^{(i)}, \tilde{\nu}_K^{(i)}) = \frac{1}{N} \sum_{i=1}^N \varepsilon_K(\mu^{(i)}). \quad (17)$$

Remark 3.5. Proposition 3.4 and the consistency results (16) and (17) could be extended to more general cost functions c satisfying smoothness conditions such as the so-called x -regularity from [23][Definition 1].

In other words, Proposition 3.4 shows the convergence of the empirical measures $\bar{\mathbb{P}}_K^N$ and $\tilde{\mathbb{P}}_K^N$ towards \mathbb{P}^N at the rate $O(K^{-2/d})$ as K goes to $+\infty$.

Remark 3.6. By definition of optimal quantization (6), one has the inequality $W_2^2(\mu^{(i)}, \tilde{\nu}_K^{(i)}) \leq W_2^2(\mu^{(i)}, \bar{\nu}_K^{(i)})$ for all $1 \leq i \leq N$. Therefore, we deduce from Proposition 3.4 that $\mathcal{W}_2^2(\tilde{\mathbb{P}}_K^N, \mathbb{P}^N) \leq \mathcal{W}_2^2(\bar{\mathbb{P}}_K^N, \mathbb{P}^N)$. Hence, $\tilde{\mathbb{P}}_K^N$ is a better approximation of \mathbb{P}^N than $\bar{\mathbb{P}}_K^N$. Still, the rates of convergence of $\mathcal{W}_2^2(\tilde{\mathbb{P}}_K^N, \mathbb{P}^N)$ and $\mathcal{W}_2^2(\bar{\mathbb{P}}_K^N, \mathbb{P}^N)$ are both scaling as $O(K^{-2/d})$. Moreover, when the $\mu^{(i)}$'s are discrete, mean-measure quantization has computational advantages over optimal quantization of each input measure for moderate to large values of N (see Section 4.1).

Remark 3.7. We simplify notation by denoting $\tilde{\nu}_K^{(i)}$ (resp. $\tilde{\mathbb{P}}_K^N$), defined in (11), and $\bar{\nu}_K^{(i)}$ (resp. $\bar{\mathbb{P}}_K^N$) defined in (14), by $\nu_K^{(i)}$ (resp. \mathbb{P}_K^N). We also write $\varepsilon_K = \mathcal{W}_2^2(\mathbb{P}_K^N, \mathbb{P}^N)$, where $\varepsilon_K = \frac{1}{N} \sum_{i=1}^N \varepsilon_K(\mu^{(i)})$ in the case of optimal quantization of each input measure, and $\varepsilon_K = \varepsilon_K(\bar{\mu})$ in the case of mean-measure quantization.

Since \mathcal{X} is a compact set, so is the metric space $(\mathcal{P}(\mathcal{X}), W_2)$ [44][Remark 6.17]. Then, by [40][Theorem 5.9], $\mathcal{W}_2(\mathbb{P}_K^N, \mathbb{P}) \rightarrow 0$ if and only if $\mathbb{P}_K^N \rightarrow \mathbb{P}^N$ in the sense of weak convergence of distributions, or in other words for any bounded continuous function $f : \mathcal{P}(\mathcal{X}) \rightarrow \mathbb{R}$, it holds that $\int f(\nu) d\mathbb{P}_K^N(\nu) \xrightarrow{K \rightarrow +\infty} \int f(\mu) d\mathbb{P}^N(\mu)$. Proposition 3.4 implies the consistency of numerous statistics computed from the quantized measures $(\nu_K^{(i)})_{1 \leq i \leq N}$ and also allows to show convergence in the MMD sense.

Corollary 3.8. *One has*

$$\frac{1}{N} \sum_{i=1}^N \text{MMD}^2(\mu^{(i)}, \nu_K^{(i)}) \leq \varepsilon_K \xrightarrow{K \rightarrow \infty} 0. \quad (18)$$

3.2 Statistics from the quantized measures

We focus here on how statistics computed from the quantized measures $(\nu_K^{(i)})_{i=1}^N$, defined either by (11) or (14), relate to statistics from the input measures $(\mu^{(i)})_{i=1}^N$.

3.2.1 Wasserstein barycenter

A first example consists in proving that a Wasserstein barycenter [1] of the $(\nu_K^{(i)})_{1 \leq i \leq N}$ converges towards the unique Wasserstein barycenter of the measures $(\mu^{(i)})_{1 \leq i \leq N}$ when at least one of them is a.c.

Proposition 3.9. *Let ν_K^{bar} be a Wasserstein barycenter of $(\nu_K^{(i)})_{1 \leq i \leq N}$ that is*

$$\nu_K^{\text{bar}} \in \underset{\nu \in \mathcal{P}(\mathcal{X})}{\operatorname{argmin}} \frac{1}{N} \sum_{i=1}^N W_2^2(\nu, \nu_K^{(i)}).$$

If at least one of the measures $(\mu^{(i)})_{1 \leq i \leq N}$ is a.c., then ν_K^{bar} converges to the unique Wasserstein barycenter μ^{bar} of $(\mu^{(i)})_{1 \leq i \leq N}$ in the Wasserstein sense as $K \rightarrow +\infty$.

3.2.2 Statistical dispersion

For a set of measures $\mu = (\mu^{(i)})_{i=1}^N$, we define its dispersion as the sum of squares $\text{SS}(\mu) = \frac{1}{N^2} \sum_{i,j=1}^N W_2^2(\mu^{(i)}, \mu^{(j)})$. The following shows that $\text{SS}(\nu_K)$, for $\nu_K = (\nu_K^{(i)})_{i=1}^N$, is controlled by $\text{SS}(\mu)$ and the quantization error ε_K defined in Remark 3.7.

Proposition 3.10. *One has that for any $\lambda > 0$,*

$$\text{SS}(\nu_K) \leq (1 + 2/\lambda) \text{SS}(\mu) + (4 + 2\lambda) \varepsilon_K.$$

Guaranteeing that the pairwise distance $W_2(\nu_K^{(i)}, \nu_K^{(j)})$ is a good approximation of $W_2(\mu^{(i)}, \mu^{(j)})$ is essential as many machine learning tasks rely on comparing pairs of data. For mean-measure quantization (12), we provide below a result on pairwise distances when the input measures are all a.c., which only depends on the quantization.

Proposition 3.11. *Suppose that the probability measures $(\mu^{(i)})_{i=1}^N$ are a.c. Then, one has*

$$W_2^2(\bar{\nu}_K^{(i)}, \bar{\nu}_K^{(j)}) \leq 3W_2^2(\mu^{(i)}, \mu^{(j)}) + 6 \max_{1 \leq k \leq K} \text{diam}(V_k),$$

with $\text{diam}(V_k) = \max_{x,y \in V_k} \|x - y\|^2$ and $(V_k)_{k=1}^K$ the Voronoï cells (15) obtained from the K -points quantization of $\bar{\mu}$.

The following lemma provides an upper bound on the term $\max_k \text{diam}(V_k)$ in Proposition 3.11 in the special case where the support of $\bar{\mu}$ is included in $[0, 1]^d$. This bound depends on the number of centers K and the ambient dimension d , and holds true for either discrete or continuous support.

Lemma 3.12. *Suppose that the (discrete or continuous) support of the mean measure $\bar{\mu}$ is included in $[0, 1]^d$ and let $(V_k)_{k=1}^K$ be the Voronoï cells of the quantization of $\bar{\mu}$. Then,*

$$\max_{1 \leq k \leq K} \text{diam}(V_k) \leq \frac{d}{\lfloor \sqrt[d]{K} \rfloor^2}.$$

3.2.3 Clustering performances

We now show that both quantization methods preserve the clustering structure of the input measures. To this end, let us assume that each measure $\mu^{(i)}$ has a label $1 \leq l \leq L$. We note I_l the set of indices such that $\forall i \in I_l, \mu^{(i)}$ has label l , and N_l its cardinal. When clustering data, one usually aims at minimizing the within-class variance WCSS for a cluster l and maximizing the between-class variance BCSS for clusters l_1 and l_2 , where for a set of measure $\mu = (\mu^{(i)})_{i=1}^N$,

$$\begin{aligned} \text{WCSS}(l, \mu) &= \frac{1}{N_l^2} \sum_{i,j \in I_l} W_2^2(\mu^{(i)}, \mu^{(j)}), \\ \text{BCSS}(l_1, l_2, \mu) &= \frac{1}{N_{l_1} N_{l_2}} \sum_{\substack{i_1 \in I_{l_1} \\ i_2 \in I_{l_2}}} W_2^2(\mu^{(i_1)}, \mu^{(i_2)}). \end{aligned}$$

The next result gives a bound on clustering performances of the quantized measures, and is illustrated in Section 4.

Proposition 3.13. *For a given class $1 \leq l \leq L$, one has*

$$\text{WCSS}(l, \nu_K) \leq 3\text{WCSS}(l, \mu) + \frac{6N}{N_l} \varepsilon_K. \quad (19)$$

For two distinct classes l_1 and l_2 , one has that

$$\text{BCSS}(l_1, l_2, \nu_K) \geq \frac{1}{3} \text{BCSS}(l_1, l_2, \mu) - \left(\frac{N}{N_{l_1}} + \frac{N}{N_{l_2}} \right) \varepsilon_K, \quad (20)$$

where ε_K is the quantization error defined in Remark 3.7.

3.3 Machine learning from the quantized measures

We consider here the embeddings of measures into a Hilbert space using either LOT or KME in Section 2. We focus on comparing the performances of machine learning methods after such embeddings of the input measures $(\mu^{(i)})_{i=1}^N$ and their quantized versions $(\nu_K^{(i)})_{i=1}^N$. To this end, we compare the Gram matrices of the pairwise inner-products between the set of embedded measures. Indeed, these matrices play a crucial role in various machine learning tasks [22] such as PCA or Linear Discriminant Analysis (LDA), that rely on the diagonalization of the covariance operator of data in a Hilbert space, which is equivalent to diagonalizing the Gram matrix of inner-products as recalled in Appendix B.

In the following, for a given embedding ϕ of probability measures into a Hilbert space \mathcal{H} equipped with the inner-product $\langle \cdot, \cdot \rangle_{\mathcal{H}}$, we will denote G_{μ}^{ϕ} and $G_{\nu_K}^{\phi}$ the $N \times N$ Gram matrices associated with $(\mu^{(i)})_{1 \leq i \leq N}$ and $(\nu_K^{(i)})_{1 \leq i \leq N}$ respectively, with entries

$$(G_{\mu}^{\phi})_{ij} = \langle \phi(\mu^{(i)}), \phi(\mu^{(j)}) \rangle_{\mathcal{H}}, \text{ and } (G_{\nu_K}^{\phi})_{ij} = \langle \phi(\nu_K^{(i)}), \phi(\nu_K^{(j)}) \rangle_{\mathcal{H}},$$

and $\|\cdot\|_F$ the Frobenius matrix norm.

Proposition 3.14. (i) We denote G_{μ}^{LOT} and $G_{\nu_K}^{\text{LOT}}$ the Gram matrices corresponding to the LOT embedding $\phi : \sigma \mapsto T_{\rho}^{\sigma} - \text{id}$, where $\rho \in \mathcal{P}(\mathcal{X})$ is any a.c. reference measure with support included in the compact set $\mathcal{X} \subset \mathbb{R}^d$. Assume that the Brenier maps $T_{\rho}^{\mu^{(i)}}$ are L -Lipschitz for all $1 \leq i \leq N$. Then, we have that

$$\frac{1}{N} \|G_{\mu}^{\text{LOT}} - G_{\nu_K}^{\text{LOT}}\|_F^2 \leq C_{N,\mathcal{X},L} \sqrt{\varepsilon_K} \quad (21)$$

where $C_{N,\mathcal{X},L}$ is a constant depending on N , the set \mathcal{X} and the Lipschitz constant L .

(ii) We note G_{μ}^{KME} and $G_{\nu_K}^{\text{KME}}$ the Gram matrices corresponding to the KME $\phi : \sigma \mapsto \int k(x, \cdot) d\sigma(x)$ for a bounded kernel function k , then:

$$\frac{1}{N} \|G_{\mu}^{\text{KME}} - G_{\nu_K}^{\text{KME}}\|_F^2 \leq C_{N,k} \varepsilon_K \quad (22)$$

where $C_{N,k}$ is a constant depending on N and the kernel k .

As a consequence of Proposition 3.14, we have that a functional PCA of the maps $(\phi(\nu_K^{(i)}))_{i=1}^N$ in a certain Hilbert space is consistent (as $K \rightarrow +\infty$) with the PCA of the maps $(\phi(\mu^{(i)}))_{i=1}^N$ in the same Hilbert space.

4 Numerical experiments

In our experiments, we distinguish the two quantization approaches : \tilde{K} -LOT and \tilde{K} -KME refer to the LOT embedding and KME of $(\tilde{\nu}_K^{(i)})_{i=1}^K$ obtained from the quantization of each $\mu^{(i)}$, while \overline{K} -LOT and \overline{K} -KME refer to the LOT embedding and KME of $(\overline{\nu}_K^{(i)})_{i=1}^K$ obtained from the mean-measure quantization. Here, we aim to show that our method enables fast computation of machine learning tasks while preserving the main information of the measures.

4.1 Computational cost

For a discrete measure, we solve the quantization problem (8) using Lloyd's algorithm [29] and an initialization based on K -means++ [4]. The time complexity of the Lloyd's algorithm being linear in the number of data points [21], it follows that for discrete measures μ_1, \dots, μ_N supported on m_1, \dots, m_N points respectively, the computational cost for constructing the quantized measures $(\nu_K^{(i)})_{i=1}^K$ by either optimal quantization of each input measure or mean-measure quantization is $O(Kd \sum_{i=1}^N m_i)$. Nevertheless, as the support of $\bar{\mu}$ is very large in applications, the mean measure quantization can be done on $\frac{1}{N} \sum_{i=1}^N m_i$ points randomly sampled from $\bar{\mu}$, leading to optimal locations $\bar{x}_1, \dots, \bar{x}_K$ similar to those of the K -quantization of the entire support of $\bar{\mu}$. Then, the computation cost of mean-measure quantization becomes $O(Kd \frac{1}{N} \sum_{i=1}^N m_i)$ and is advantageous over the optimal quantization of each input measure.

In order to compute the LOT embedding, we solve the discrete OT problem (2) between m_0 samples of ρ and m_i samples of $\mu^{(i)}$ using a standard OT solver [15, 36]. Then, as the optimal map $T_\rho^{\mu^{(i)}}$ in (5) might not exist, it is classical [13] to compute an approximation through barycentric projection of an optimal transport plan, solution of (2). The overall computational of \bar{K} -LOT when using m_0 samples from the reference measure ρ is thus $O(Kd \frac{1}{N} \sum_{i=1}^N m_i) + O(N(K + M)Km_0 \log(K + m_0))$ which is significantly smaller than the one of LOT from the raw input measures that scales as $O(\sum_{i=1}^N (m_i + m_0)m_i m_0 \log(m_i + m_0))$.

Similarly, the computational cost of K -KME to construct the Gram matrix $G_{\nu_K}^{\text{KME}}$ is $O(Kd \frac{1}{N} \sum_{i=1}^N m_i) + O(N^2 K^2)$ that is much cheaper than the cost of computing G_μ^{KME} from the raw data that scales as $O(\sum_{i,j=1}^N m_i m_j)$.

4.2 Synthetic dataset : shifts and scalings of a reference measure

We consider input measures that are shifts and scalings of a given a.c. compactly supported measure ρ , that is:

$$\mu^{(i)} = (\Sigma_i^{1/2} \text{id} + b_i)_\# \rho, \quad (23)$$

where $\Sigma_i \in \mathbb{R}^{d \times d}$ is a positive semi-definite matrix and $b_i \in \mathbb{R}^d$. We choose $X \sim \rho$ such that $X = R \frac{Z}{\|Z\|}$, with $R \sim \text{Unif}([0, 1])$ and $Z \sim \mathcal{N}(0, I_d)$. In that case, we have an explicit formulation of the pairwise inner-products induced by LOT embedding and KME, see Proposition C.1 in Appendix C. We can therefore exactly compute the so-called *true matrix* G_μ^ϕ . We numerically sample the distributions $\mu^{(i)}$'s in the following way : for each $1 \leq i \leq N$, we first sample m_i points $(x_j)_{1 \leq j \leq m_i}$ from the measure ρ by sampling $z_j \sim \mathcal{N}(0, I_d)$ and $r_j \sim \text{Unif}([0, 1])$ and computing $x_j = r_j \frac{z_j}{\|z_j\|}$. This allows to sample points from the unit ball in \mathbb{R}^d . Samples from $\mu^{(i)}$ are then obtained by the pushforward operation in (23).

We first compare in Figure 2 the computational costs of both quantization methods and observe that the mean-measure quantization approach is faster. In Figure 3 (resp. Figure 4 in Appendix C), we visualize the projections on the first two components of PCA

for K -LOT (resp. K -KME) of both quantization methods and compare them to the PCA computed from the true Gram matrices G_μ^ϕ computed in Proposition C.1. We observe that even with a small value $K = 32$, the PCA visualizations on quantized embedded measures mimic the ones on raw embedded input measures.

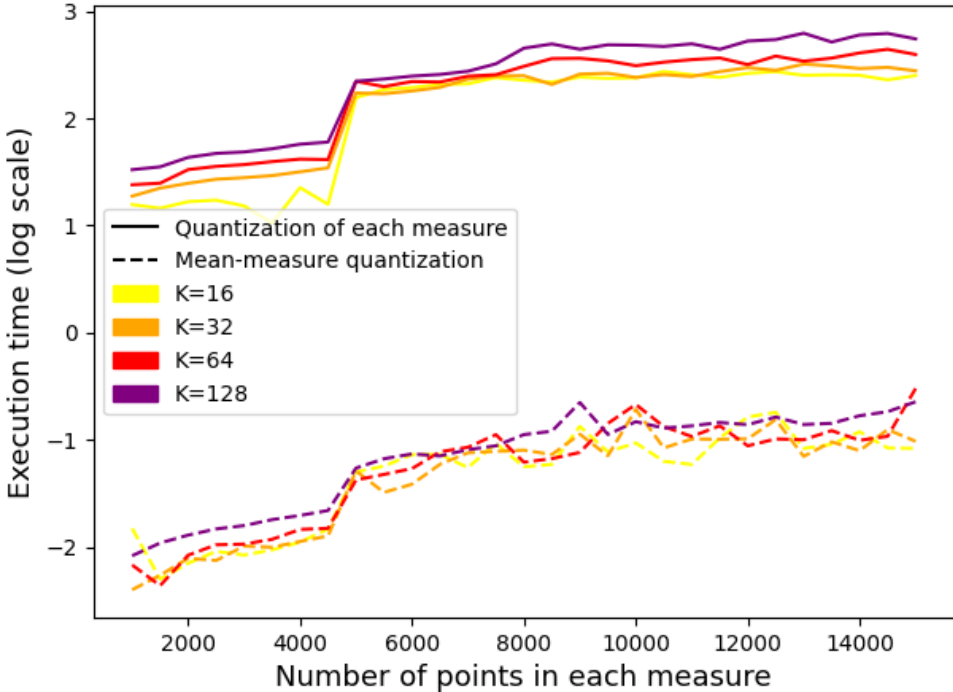


Figure 2: **Synthetic dataset on shifts and scalings.** Evaluation time for the computation of the two quantization steps for $d = 2$ and for different values of K .

4.3 Flow cytometry dataset

In this section, we use flow cytometry datasets provided in [43] and publicly available in Mendeley Data to illustrate the suitability of our method through a classification task. We have $N = 108$ cytometry measures (or point cloud) which come from two different health care centers : Marburg and Dresden. In Marburg, the data consists of diagnostic samples of peripheral blood (pB), healthy bone marrow (BM), or leukemic bone marrow. The Dresden dataset consists of diagnostic samples of peripheral blood and healthy bone marrow. Two types of labels can be distinguished: data are differentiated either by the healthcare centers from which they were analyzed, or by their types (e.g., peripheral blood, healthy bone marrow, or leukemic bone marrow). Each measure contains from

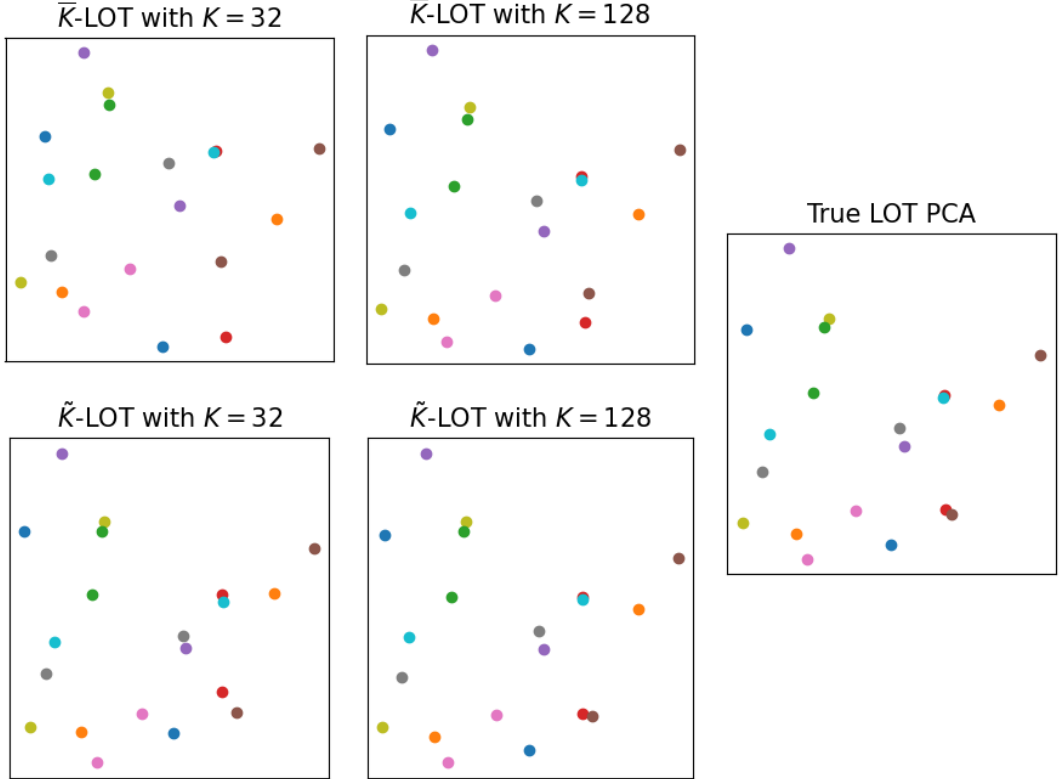


Figure 3: **Synthetic dataset on shifts and scalings.** Projection of the data onto the first two components of PCA after \bar{K} -LOT (top) and \tilde{K} -LOT (bottom) and comparison to the LOT PCA (right) computed from the true Gram matrix (see Prop.C.1).

100,000 to 1,000,000 points in dimension $d = 10$, which prevents the use of classical OT, that is, without a quantization step. For K -LOT, we sample $m_0 = 1000$ points from the reference measure chosen as the uniform measure on $[0, 1]^d$ and for K -KME, we use the Gaussian kernel with bandwidth parameter $\sigma = 1$. The embedded measures live in a high-dimensional Hilbert space (e.g. with K -LOT and $K = 128$, the ambient space is \mathbb{R}^{1280}). In order to keep the most relevant information, we perform a 10-components PCA on the embedded data with respect to the proper Hilbert space \mathcal{H} . Then, we train two classifiers (one for each type of label) on 75% of the data and test the results on the remaining data with LDA. We compare our method with random Fourier features (RFF) [38], which allow to efficiently map raw probability measures into the linear space \mathbb{R}^s , where s is a parameters that has to be chosen. Note that RFF then approximate the KME. Accuracy scores are displayed in Table 1. The quantization methods achieve in particular perfect accuracy scores for predicting the health care center (denoted as LAB)

Table 1: **Flow cytometry dataset.** Classification accuracies and execution times for LDA after 10-component PCA on K -LOT, K -KME with both quantization methods and KME with RFF.

K -LOT/ \tilde{K} -LOT				K -KME/ \tilde{K} -KME				KME WITH RFF			
K	ACCURACY (LAB)	ACCURACY (TYPE)	TIME (s)	ACCURACY (LAB)	ACCURACY (TYPE)	TIME (s)	s	ACCURACY (LAB)	ACCURACY (TYPE)	TIME (s)	
16	100/100	85/81	23/103	100/100	83/69	15/96	16	73	44	4524	
32	100/100	94/81	25/166	100/100	83/69	34/174	32	75	44	4701	
64	100/100	94/81	30/281	100/100	85/69	105/358	64	83	52	5035	
128	100/100	88/81	32/555	100/100	77/71	387/909	128	92	44	5676	

Table 2: **Earth image dataset.** LDA classification accuracy on the Airbus dataset after 10-component PCA on K -LOT and K -KME with both quantization methods.

K -LOT/ \tilde{K} -LOT			K -KME/ \tilde{K} -KME		
K	ACCURACY	TIME (s)	ACCURACY	TIME	
16	88/88	15/228	76/68	219/732	
32	89/89	17/249	67/67	2792/2247	
64	89/88	20/305	68/68	7958/9246	
128	88/88	32/390	67/66	31765/32287	

in only a few minutes. The KME computed with RFF reaches lower accuracy scores and is clearly slower than both quantization methods. Comparing the quantization methods, we observe that the classifier performs better on mean-measure quantization than on the quantization of each measure whereas the latter is roughly ten times slower than the former.

Additionally, we visualize the projections of the data on the first components of PCA in Figures 5 and 6 of the Appendix C. In these figures, it is clear that the representations stabilize when $K \geq 32$. This shows that our K -quantization step gives good results even for small values of K . We also observe that the mean-measure quantization and the quantization of each measure yield similar results.

4.4 Earth image dataset

We perform similar experiments on a set of images provided by the Airbus company. The dataset consists in $N = 1000$ images of size 128×128 captured by a SPOT satellite. The images are divided into two categories : those with the presence of a wind turbine and those without, see Figures 7a and 7b in Appendix C. Each image is viewed as a discrete probability distribution on the RGB space, that is each pixel is represented by a point in \mathbb{R}^3 . The size N of the dataset as well as the number of pixels ($m_i = 128^2$) prevents from directly computing either LOT or KME. We therefore carry out supervised classification from both embeddings and both quantization methods. For $K \in \{16, 32, 64, 128\}$, we implement

K -LOT with reference measure the uniform measure on $[0, 1]^3$ sampled on $m_0 = 1000$ points, and K -KME with the Gaussian kernel with bandwidth parameter $\sigma = 100$. After the embeddings, we perform PCA and retain only the first 10 components, on which we train an LDA classifier using 75% of the data and test it on the remaining 25%. We obtain the accuracies and execution times displayed in Table 2. Both quantization methods achieve similar accuracy results while mean-measure quantization is approximately ten times faster than the quantization of each measure.

5 Conclusion

In this work, we have proposed to handle machine learning tasks of a set of probability distributions by leveraging two different K -quantization approaches that both approximate the input distributions at the asymptotic rate $O(K^{-2/d})$. We proved theoretically that mean-measure quantization and quantization of each measure allow the construction of scalable and consistent embeddings of the probability measures into Hilbert spaces, while numerical experiments highlight the efficiency and accuracy of the former.

References

- [1] Martial Aguech and Guillaume Carlier. Barycenters in the Wasserstein space. *SIAM Journal on Mathematical Analysis*, 43(2):904–924, 2011.
- [2] Luigi Ambrosio, Nicola Gigli, and Giuseppe Savaré. *Gradient flows: in metric spaces and in the space of probability measures*. Springer Science & Business Media, 2008.
- [3] Ery Arias-Castro and Wanli Qiao. Embedding distribution data. *Annals of Statistics*, To be published, 2024.
- [4] David Arthur and Sergei Vassilvitskii. k-means++: the advantages of careful seeding. In *SODA '07: Proceedings of the eighteenth annual ACM-SIAM symposium on Discrete algorithms*, pages 1027–1035, 2007.
- [5] François Bachoc, Alexandra Suvorikova, David Ginsbourger, Jean-Michel Loubes, and Vladimir Spokoiny. Gaussian processes with multidimensional distribution inputs via optimal transport and Hilbertian embedding. *Electronic Journal of Statistics*, 14(2):2742 – 2772, 2020.
- [6] François Bachoc, Fabrice Gamboa, Jean-Michel Loubes, and Nil Venet. A Gaussian process regression model for distribution inputs. *IEEE Transactions on Information Theory*, 64(10):6620–6637, 2018.
- [7] Gaspard Beugnot, Aude Genevay, Kristjan Greenewald, and Justin Solomon. Improving approximate optimal transport distances using quantization. In *Uncertainty in artificial intelligence*, pages 290–300. PMLR, 2021.

- [8] Jérémie Bigot, Raúl Gouet, Thierry Klein, and Alfredo López. Geodesic PCA in the Wasserstein space by convex PCA. *Annales de l'Institut Henri Poincaré, Probabilités et Statistiques*, 53(1):1–26, 2017.
- [9] Yann Brenier. Polar factorization and monotone rearrangement of vector-valued functions. *Communications on pure and applied mathematics*, 44(4):375–417, 1991.
- [10] Elsa Cazelles, Vivien Seguy, Jérémie Bigot, Marco Cuturi, and Nicolas Papadakis. Geodesic PCA versus log-PCA of histograms in the Wasserstein space. *SIAM Journal on Scientific Computing*, 40(2):B429–B456, 2018.
- [11] Antoine Chatalic, Nicolas Schreuder, Lorenzo Rosasco, and Alessandro Rudi. Nyström kernel mean embeddings. In *Proceedings of the 39th International Conference on Machine Learning*, volume 162, pages 3006–3024, 2022.
- [12] Frédéric Chazal, Clément Levraud, and Martin Royer. Clustering of measures via mean measure quantization. *Electronic Journal of Statistics*, 15(1):2060 – 2104, 2021.
- [13] Nabarun Deb, Promit Ghosal, and Bodhisattva Sen. Rates of estimation of optimal transport maps using plug-in estimators via barycentric projections. *Advances in Neural Information Processing Systems*, 34:29736–29753, 2021.
- [14] Alex Delalande and Quentin Mérigot. Quantitative stability of optimal transport maps under variations of the target measure. *Duke Mathematical Journal*, 172(17):3321–3357, 2023.
- [15] Rémi Flamary, Nicolas Courty, Alexandre Gramfort, Mokhtar Z. Alaya, Aurélie Boisbunon, Stanislas Chambon, Laetitia Chapel, Adrien Corenflos, Kilian Fatras, Nemo Fournier, Léo Gautheron, Nathalie T.H. Gayraud, Hicham Janati, Alain Rakotomamonjy, Ievgen Redko, Antoine Rolet, Antony Schutz, Vivien Seguy, Danica J. Sutherland, Romain Tavenard, Alexander Tong, and Titouan Vayer. Pot: Python optimal transport. *Journal of Machine Learning Research*, 22(78):1–8, 2021.
- [16] Erell Gachon, Jérémie Bigot, Elsa Cazelles, Aguirre Mimoun, and Jean-Philippe Vial. Low dimensional representation of multi-patient flow cytometry datasets using optimal transport for minimal residual disease detection in leukemia. *arXiv preprint arXiv:2407.17329*, 2024.
- [17] Nicola Gigli. On Hölder continuity-in-time of the optimal transport map towards measures along a curve. *Proceedings of the Edinburgh Mathematical Society*, 54(2):401–409, 2011.
- [18] Frédéric Gournay, Jonas Kahn, and Léo Lebrat. Differentiation and regularity of semi-discrete optimal transport with respect to the parameters of the discrete measure. *Numer. Math.*, 141(2):429–453, 2019.
- [19] Siegfried Graf and Harald Luschgy. *Foundations of quantization for probability distributions*. Springer Science & Business Media, 2000.

- [20] Arthur Gretton, Karsten M. Borgwardt, Malte J. Rasch, Bernhard Schölkopf, and Alexander Smola. A kernel two-sample test. *Journal of Machine Learning Research*, 13(25):723–773, 2012.
- [21] J. A. Hartigan and M. A. Wong. Algorithm as 136: A k-means clustering algorithm. *Journal of the Royal Statistical Society. Series C (Applied Statistics)*, 28(1):100–108, 1979.
- [22] Thomas Hofmann, Bernhard Schölkopf, and Alexander J. Smola. Kernel methods in machine learning. *The Annals of Statistics*, 36(3):1171 – 1220, 2008.
- [23] Antoine Houdard, Arthur Leclaire, Nicolas Papadakis, and Julien Rabin. On the gradient formula for learning generative models with regularized optimal transport costs. *Transactions on Machine Learning Research Journal*, 2023.
- [24] Abdelwahed Khamis, Russell Tsuchida, Mohamed Tarek, Vivien Rolland, and Lars Petersson. Scalable optimal transport methods in machine learning: A contemporary survey. *IEEE Transactions on Pattern Analysis and Machine Intelligence*, 2024.
- [25] Benoît Kloeckner. Approximation by finitely supported measures. *ESAIM: Control, Optimisation and Calculus of Variations*, 18(2):343–359, 2012.
- [26] Soheil Kolouri, Se Rim Park, Matthew Thorpe, Dejan Slepcev, and Gustavo K. Rohde. Optimal mass transport: Signal processing and machine-learning applications. *IEEE Signal Processing Magazine*, 34(4):43–59, 2017.
- [27] Thibaut Le Gouic and Jean-Michel Loubes. Existence and consistency of Wasserstein barycenters. *Probability Theory and Related Fields*, 168:901–917, 2017.
- [28] Yating Liu and Gilles Pagès. Convergence rate of optimal quantization and application to the clustering performance of the empirical measure. *Journal of Machine Learning Research*, 21(86):1–36, 2020.
- [29] Stuart Lloyd. Least squares quantization in PCM. *IEEE transactions on information theory*, 28(2):129–137, 1982.
- [30] Katherine M McKinnon. Flow cytometry: an overview. *Current protocols in immunology*, 120(1):5–1, 2018.
- [31] Dimitri Meunier, Massimiliano Pontil, and Carlo Ciliberto. Distribution regression with sliced Wasserstein kernels. In *Proceedings of the 39th International Conference on Machine Learning*, volume 162 of *Proceedings of Machine Learning Research*, pages 15501–15523, 2022.
- [32] Eduardo Fernandes Montesuma, Fred Maurice Ngol, Mboula, and Antoine Souloumiac. Recent advances in optimal transport for machine learning. *IEEE Transactions on Pattern Analysis and Machine Intelligence*, pages 1–20, 2024.

- [33] Caroline Moosmüller and Alexander Cloninger. Linear optimal transport embedding: provable Wasserstein classification for certain rigid transformations and perturbations. *Information and Inference: A Journal of the IMA*, 12(1):363–389, 2023.
- [34] Krikamol Muandet, Kenji Fukumizu, Bharath Sriperumbudur, Bernhard Schölkopf, et al. Kernel mean embedding of distributions: A review and beyond. *Foundations and Trends® in Machine Learning*, 10(1-2):1–141, 2017.
- [35] Gilles Pagès. Introduction to vector quantization and its applications for numerics. *ESAIM: proceedings and surveys*, 48:29–79, 2015.
- [36] Gabriel Peyré and Marco Cuturi. Computational optimal transport: With applications to data science. *Foundations and Trends® in Machine Learning*, 11(5-6):355–607, 2019.
- [37] Barnabas Poczos, Aarti Singh, Alessandro Rinaldo, and Larry Wasserman. Distribution-free distribution regression. In *Proceedings of the Sixteenth International Conference on Artificial Intelligence and Statistics*, volume 31 of *Proceedings of Machine Learning Research*, pages 507–515, 2013.
- [38] Ali Rahimi and Benjamin Recht. Random features for large-scale kernel machines. *Advances in neural information processing systems*, 20, 2007.
- [39] Martin Royer, Frédéric Chazal, Clément Levraud, Yuhei Umeda, and Yuichi Ike. Atol: measure vectorization for automatic topologically-oriented learning. In *International Conference on Artificial Intelligence and Statistics*, pages 1000–1008. PMLR, 2021.
- [40] Filippo Santambrogio. Optimal transport for applied mathematicians. *Birkhäuser, NY*, 55(58-63):94, 2015.
- [41] Vivien Seguy and Marco Cuturi. Principal geodesic analysis for probability measures under the optimal transport metric. *Advances in Neural Information Processing Systems*, 28, 2015.
- [42] Zoltán Szabó, Bharath K. Sriperumbudur, Barnabás Póczos, and Arthur Gretton. Learning theory for distribution regression. *Journal of Machine Learning Research*, 17(152):1–40, 2016.
- [43] Michael C Thrun, Jörg Hoffmann, Maximilian Röhnert, Malte von Bonin, Uta Oelschlägel, Cornelia Brendel, and Alfred Ultsch. Flow cytometry datasets consisting of peripheral blood and bone marrow samples for the evaluation of explainable artificial intelligence methods. *Data in Brief*, 43:108382, 2022.
- [44] Cédric Villani. *Optimal transport: old and new*, volume 338. Springer, 2009.
- [45] Wei Wang, Dejan Slepčev, Saurav Basu, John A. Ozolek, and Gustavo K. Rohde. A linear optimal transportation framework for quantifying and visualizing variations in sets of images. *International journal of computer vision*, 101:254–269, 2013.

A Proofs of the main results

Lemma A.1. *Let $X = (x_1, \dots, x_K) \in F_K$ the set of distinct points and consider the Voronoï partition*

$$\tilde{V}_{x_1} = V_{x_1} \text{ and } \tilde{V}_{x_k} = V_{x_k} \setminus \bigcup_{j < k} \tilde{V}_{x_j} \quad \text{for } k \geq 2,$$

where we recall that

$$V_{x_k} = \{y \in \mathbb{R}^d \mid \forall \ell \neq k, \|x_k - y\|^2 \leq \|x_\ell - y\|^2\}.$$

Then, for any probability measure $\mu \in \mathcal{P}(\mathcal{X})$, one has that

$$\begin{aligned} \min_{a \in \Sigma_K} W_2^2\left(\mu, \sum_{k=1}^K a_k \delta_{x_k}\right) &= W_2^2\left(\mu, \sum_{k=1}^K \mu(\tilde{V}_{x_k}) \delta_{x_k}\right) \\ &= \sum_{k=1}^K \int_{\tilde{V}_{x_k}} \|x_k - y\|^2 d\mu(y) \\ &= \int_{\mathbb{R}^d} \min_{1 \leq k \leq K} \{\|x_k - y\|^2\} d\mu(y). \end{aligned}$$

Proof of Lemma A.1. Let $X = (x_1, \dots, x_K) \in F_K$. From the dual formulation of the Kantorovich problem (see e.g. [44]), we have that, for any $a \in \Sigma_K$,

$$\begin{aligned} W_2^2\left(\mu, \sum_{k=1}^K a_k \delta_{x_k}\right) &= \sup_{\beta \in \mathbb{R}^K} \sum_{k=1}^K a_k \beta_k + \int_{\mathbb{R}^d} \left(\min_{1 \leq k \leq K} \{\|x_k - y\|^2 - \beta_k\} \right) d\mu(y) \\ &\geq \int_{\mathbb{R}^d} \min_{1 \leq k \leq K} \{\|x_k - y\|^2\} d\mu(y), \end{aligned} \tag{24}$$

where the above inequality is obtain by taking $\beta_k = 0$ for all $1 \leq k \leq K$. Then, since $X = (x_1, \dots, x_K) \in F_K$, one has that $(\tilde{V}_{x_k})_{1 \leq k \leq K}$ is a partition of \mathbb{R}^d , and we may define

$$T_K(y) = \sum_{k=1}^K x_k \mathbb{1}_{\tilde{V}_{x_k}}(y) \quad y \in \mathbb{R}^d,$$

that is a mapping from \mathbb{R}^d to X . Introducing the probability measure $\mu_K = \sum_{k=1}^K \mu(\tilde{V}_{x_k}) \delta_{x_k}$, it is not difficult to see that $T_K \# \mu = \mu_K$ where the notation $T \# \mu$ denotes the push-forward of a measure μ by the mapping T . Now, we let $\pi_K = (\text{id} \times T_K) \# \mu$ that obviously belongs to the set of transport plans $\Pi(\mu, \mu_K)$. From the definition of the Voronoï partition $(\tilde{V}_{x_k})_{1 \leq k \leq K}$, one can than check that, for any $y \in \mathbb{R}^d$, (see e.g. [35])

$$\|y - T_K(y)\|^2 = \min_{1 \leq k \leq K} \{\|x_k - y\|^2\}.$$

Consequently, we obtain the following equalities

$$\int_{\mathcal{X} \times \mathcal{X}} \|x - y\|^2 d\pi_K(x, y) = \int_{\mathbb{R}^d} \|y - T_K(y)\|^2 d\mu(y) = \int_{\mathbb{R}^d} \min_{1 \leq k \leq K} \{\|x_k - y\|^2\} d\mu(y).$$

Inserting the above equality into (24), we thus have that, for any $a \in \Sigma_K$,

$$W_2^2(\mu, \sum_{k=1}^K a_k \delta_{x_k}) \geq \int_{\mathcal{X} \times \mathcal{X}} \|x - y\|^2 d\pi_K(x, y).$$

Since $W_2^2(\mu, \mu_K) = \min_{\pi \in \Pi(\mu, \mu_K)} \int_{\mathcal{X} \times \mathcal{X}} \|x - y\|^2 d\pi(x, y)$, we directly obtain from the above inequality that $W_2^2(\mu, \mu_K) = \int_{\mathcal{X} \times \mathcal{X}} \|x - y\|^2 d\pi_K(x, y)$, which implies

$$\min_{a \in \Sigma_K} W_2^2\left(\mu, \sum_{k=1}^K a_k \delta_{x_k}\right) = W_2^2(\mu, \mu_K) = \int_{\mathbb{R}^d} \|y - T_K(y)\|^2 d\mu(y) = \int_{\mathbb{R}^d} \min_{1 \leq k \leq K} \{\|x_k - y\|^2\} d\mu(y),$$

which concludes the proof. \square

Proof of Proposition 3.1. Let $X \in F_K$. Applying Lemma A.1, we obtain that, for any $1 \leq i \leq N$,

$$\min_{a^{(i)} \in \Sigma_K} W_2^2\left(\mu^{(i)}, \sum_{k=1}^K a_k^{(i)} \delta_{x_k}\right) = W_2^2\left(\mu, \sum_{k=1}^K \mu^{(i)}(\tilde{V}_{x_k}) \delta_{x_k}\right) = \sum_{k=1}^K \int_{\tilde{V}_{x_k}} \|x_k - y\|^2 d\mu^{(i)}(y),$$

and thus we have that

$$\begin{aligned} \min_{a \in (\Sigma_K)^N} \frac{1}{N} \sum_{i=1}^N W_2^2\left(\mu^{(i)}, \sum_{k=1}^K a_k^{(i)} \delta_{x_k}\right) &= \frac{1}{N} \sum_{i=1}^N W_2^2\left(\mu, \sum_{k=1}^K \mu^{(i)}(\tilde{V}_{x_k}) \delta_{x_k}\right) \\ &= \frac{1}{N} \sum_{i=1}^N \sum_{k=1}^K \int_{\tilde{V}_{x_k}} \|x_k - y\|^2 d\mu^{(i)}(y) \\ &= \sum_{k=1}^K \int_{\tilde{V}_{x_k}} \|x_k - y\|^2 d\bar{\mu}(y) \\ &= W_2^2\left(\bar{\mu}, \sum_{k=1}^K \bar{\mu}(\tilde{V}_{x_k}) \delta_{x_k}\right) \\ &= \int_{\mathbb{R}^d} \min_{1 \leq k \leq K} \{\|x_k - y\|^2\} d\bar{\mu}(y), \end{aligned}$$

where we again apply Lemma A.1 to derive the last equality above. Finally, from the assumption that the cardinality of the support of $\bar{\mu}$ is larger than K , we obtain from [28][Proposition 2] that

$$\min_{X \in F_K} W_2^2\left(\bar{\mu}, \sum_{k=1}^K \bar{\mu}(\tilde{V}_{x_k}) \delta_{x_k}\right) = \min_{X \in (\mathbb{R}^d)^K} W_2^2\left(\bar{\mu}, \sum_{k=1}^K \bar{\mu}(\tilde{V}_{x_k}) \delta_{x_k}\right)$$

which concludes the proof. \square

Proof of Proposition 3.4. For a fixed $N \geq 1$, since \mathbb{P}^N , $\bar{\mathbb{P}}_K^N$ and $\tilde{\mathbb{P}}_K^N$ are discrete uniform measures of the same size, one can actually restrict the search of an optimal plan in (4) as that of finding an optimal permutation $\sigma \in \text{Perm}(N)$ see e.g. [44] in the following sense:

$$\begin{aligned}\mathcal{W}_2^2(\mathbb{P}^N, \bar{\mathbb{P}}_K^N) &= \min_{\sigma \in \text{Perm}(N)} \frac{1}{N} \sum_{i=1}^N W_2^2(\mu^{(i)}, \bar{\nu}_K^{(\sigma(i))}) \\ \mathcal{W}_2^2(\mathbb{P}^N, \tilde{\mathbb{P}}_K^N) &= \min_{\sigma \in \text{Perm}(N)} \frac{1}{N} \sum_{i=1}^N W_2^2(\mu^{(i)}, \tilde{\nu}_K^{(\sigma(i))})\end{aligned}\quad (25)$$

However, for $\tilde{\nu}_K^{(i)}$, defined in (11), it follows by the definition of optimal quantization of $\mu^{(i)}$ that, for any $1 \leq j \leq N$,

$$W_2^2(\mu^{(i)}, \tilde{\nu}_K^{(i)}) \leq W_2^2(\mu^{(i)}, \tilde{\nu}_K^{(j)}). \quad (26)$$

Now for $\bar{\nu}_K^{(i)}$, defined in (14). Since $\bar{\nu}_K^{(i)}$ corresponds to the discrete probability measure supported on \bar{X} that best approximates $\mu^{(i)}$. In other words, $W_2^2(\mu^{(i)}, \bar{\nu}_K^{(i)}) \leq W_2^2(\mu^{(i)}, \sum_{k=1}^K a_k \delta_{\bar{x}_k})$ for any weight vector $a \in \Sigma_K$. In particular, we have that, for any $1 \leq j \leq N$,

$$W_2^2(\mu^{(i)}, \bar{\nu}_K^{(i)}) \leq W_2^2(\mu^{(i)}, \bar{\nu}_K^{(j)}). \quad (27)$$

Using Inequalities (26) and (27), it is then easy to see that in both cases, the optimal permutation minimizing (25) is the identity $\sigma(i) = i$ for all $1 \leq i \leq N$, and that we have

$$\mathcal{W}_2^2(\mathbb{P}^N, \bar{\mathbb{P}}_K^N) = \frac{1}{N} \sum_{i=1}^N W_2^2(\mu^{(i)}, \bar{\nu}_K^{(i)}) \quad \mathcal{W}_2^2(\mathbb{P}^N, \tilde{\mathbb{P}}_K^N) = \frac{1}{N} \sum_{i=1}^N W_2^2(\mu^{(i)}, \tilde{\nu}_K^{(i)})$$

For $\tilde{\nu}_K^{(i)}$, one immediately has that $\frac{1}{N} \sum_{i=1}^N W_2^2(\mu^{(i)}, \tilde{\nu}_K^{(i)}) = \frac{1}{N} \sum_{i=1}^N \varepsilon_K(\mu^{(i)})$. For $\bar{\nu}_K^{(i)}$, we obtain from Proposition 3.1 that

$$\frac{1}{N} \sum_{i=1}^N W_2^2(\mu^{(i)}, \bar{\nu}_K^{(i)}) = W_2^2 \left(\sum_{k=1}^K \bar{\mu}(\tilde{V}_{\bar{x}_k}) \delta_{\bar{x}_k}, \bar{\mu} \right) = \varepsilon_K$$

which concludes the proof. \square

Proof of Corollary 3.8. As MMD is an integral probability metric [20][Lemma 4], it is bounded by the 1-Wasserstein distance W_1 defined by :

$$W_1(\rho, \mu) = \min_{\pi \in \Pi(\rho, \mu)} \int_{\mathcal{X} \times \mathcal{X}} \|x - y\| d\pi(x, y). \quad (28)$$

Since $W_1 \leq W_2$ [40][Chapter 5], we thus have that $\text{MMD} \leq W_2$. Therefore,

$$\frac{1}{N} \sum_{i=1}^N \text{MMD}^2(\mu^{(i)}, \nu_K^{(i)}) \leq \varepsilon_K \xrightarrow{K \rightarrow \infty} 0. \quad (29)$$

□

Proof of Proposition 3.9. For a fixed N , and thanks to Proposition 3.4, we have that the sequence of probability measures $(\mathbb{P}_K^N)_{K \geq 1}$ such that $\mathbb{P}_K^N = \frac{1}{N} \sum_{i=1}^N \delta_{\nu_K^{(i)}} \in \mathcal{P}(\mathcal{P}(\mathcal{X}))$ converges towards \mathbb{P}^N , that is $\mathcal{W}_2(\mathbb{P}_K^N, \mathbb{P}_N) \xrightarrow{K \rightarrow \infty} 0$. Additionally, the Wasserstein barycenter of \mathbb{P}^N is unique (Proposition 3.5 in [1]) since at least one of the probability measures $\mu^{(i)}$, $1 \leq i \leq N$ is a.c. by hypothesis. Therefore, using [27][Theorem 3], we immediately obtain that the sequence of barycenters of $(\mathbb{P}_K^N)_{K \geq 1}$ converges towards the barycenter of \mathbb{P}^N in W_2 distance.

□

Proof of Proposition 3.10. From the triangle inequality, one can write:

$$W_2(\nu_K^{(i)}, \nu_K^{(j)}) \leq W_2(\nu_K^{(i)}, \mu^{(i)}) + W_2(\mu^{(i)}, \mu^{(j)}) + W_2(\mu^{(j)}, \nu_K^{(j)}).$$

From Young's inequality, $2ab \leq a^2 + b^2$ and $2ab \leq \lambda a^2 + \frac{b^2}{\lambda}$ for any $\lambda > 0$ and any real numbers a, b and c . Then it holds that :

$$(a + b + c)^2 \leq (2 + \lambda)a^2 + (2 + \lambda)c^2 + \left(1 + \frac{2}{\lambda}\right)b^2 \quad (30)$$

Squaring the triangle inequality and using (30), this yields to:

$$W_2^2(\nu_K^{(i)}, \nu_K^{(j)}) \leq (2 + \lambda)W_2^2(\nu_K^{(i)}, \mu^{(i)}) + \left(1 + \frac{2}{\lambda}\right)W_2^2(\mu^{(i)}, \mu^{(j)}) + (2 + \lambda)W_2^2(\mu^{(j)}, \nu_K^{(j)}) \quad (31)$$

We now sum inequality (31) over all $1 \leq i, j \leq N$, and divide by N^2 :

$$\text{SS}(\nu_K) = \frac{1}{N^2} \sum_{i=1}^N W_2^2(\nu_K^{(i)}, \mu^{(i)}) \leq \frac{2}{N}(2 + \lambda) \sum_{i=1}^N W_2^2(\nu_K^{(i)}, \mu^{(i)}) + \frac{1}{N^2} \left(1 + \frac{2}{\lambda}\right) \sum_{i,j=1}^N W_2^2(\mu^{(i)}, \mu^{(j)})$$

Hence, by Proposition 3.4, we obtain that $\text{SS}(\nu_K) \leq (4 + 2\lambda)\varepsilon_K + \left(1 + \frac{2}{\lambda}\right)\text{SS}(\mu)$, which concludes the proof. □

Proof of Proposition 3.11. We first recall that the dual formulation of OT between the discrete measures $\bar{\nu}_K^{(i)}$ and $\bar{\nu}_K^{(j)}$ (see e.g. [36]) is given by

$$W_2^2(\bar{\nu}_K^{(i)}, \bar{\nu}_K^{(j)}) = \max_{(\alpha, \beta) \in \Phi} \sum_{k=1}^K a_k^{(i)} \alpha_k + \sum_{k=1}^K a_k^{(j)} \beta_k \quad (32)$$

where $\Phi := \{(\alpha, \beta) \in \mathbb{R}^K \times \mathbb{R}^K \text{ such that for all } 1 \leq k, l \leq K, \alpha_k + \beta_l \leq C_{kl}\}$. Let $\alpha^{ij}, \beta^{ij} \in \mathbb{R}^K$ be optimal Kantorovich potentials for $\bar{\nu}_K^{(i)}$ and $\bar{\nu}_K^{(j)}$ in (32). We define the piecewise constant function $f^{ij} : \mathbb{R}^d \rightarrow \mathbb{R}$ such that $x \mapsto \alpha_k^{ij}$ when $x \in \overset{\circ}{V}_k$, where $\overset{\circ}{V}_k$ denotes the open interior of the Voronoï cell V_k . Similarly, $g^{ij} : y \mapsto \beta_k^{ij}$ when $y \in V_k$. Then, thanks to the absolute continuity of the $\mu^{(i)}$'s, one can write:

$$\begin{aligned}
W_2^2(\bar{\nu}_K^{(i)}, \bar{\nu}_K^{(j)}) &= \sum_{k=1}^K a_k^{(i)} \alpha_k^{ij} + \sum_{k=1}^K a_k^{(j)} \beta_k^{ij} \\
&= \sum_{k=1}^K \int_{V_k} d\mu^{(i)}(x) \alpha_k^{ij} + \sum_{k=1}^K \int_{V_k} d\mu^{(j)}(y) \beta_k^{ij} \\
&= \sum_{k=1}^K \int_{\overset{\circ}{V}_k} \alpha_k^{ij} d\mu^{(i)}(x) + \sum_{k=1}^K \int_{\overset{\circ}{V}_k} \beta_k^{ij} d\mu^{(j)}(y) \\
&= \int_{\mathbb{R}^d} f^{ij}(x) d\mu^{(i)}(x) + \int_{\mathbb{R}^d} g^{ij}(y) d\mu^{(j)}(y)
\end{aligned} \tag{33}$$

We then aim at identifying (33) with a dual formulation for OT between $\mu^{(i)}$ and $\mu^{(j)}$ with respect to some cost function $c : \mathbb{R}^d \times \mathbb{R}^d \rightarrow \mathbb{R}$ to be defined later on, where

$$\begin{aligned}
\text{OT}_c(\mu^{(i)}, \mu^{(j)}) &= \min_{\pi \in \Pi(\mu^{(i)}, \mu^{(j)})} \int c(x, y) d\pi(x, y) \\
&= \sup_{f, g: f(x) + g(y) \leq c(x, y)} \int_{\mathbb{R}^d} f(x) d\mu^{(i)}(x) + \int_{\mathbb{R}^d} g(y) d\mu^{(j)}(y).
\end{aligned} \tag{34}$$

If $x \in V_k$ and $y \in V_{k'}$, we obtain

$$\begin{aligned}
f^{ij}(x) + g^{ij}(y) &= \alpha_k^{ij} + \beta_{k'}^{ij} \\
&\leq \|x_k - x_{k'}\|^2 \\
&\leq 3\|x_k - x\|^2 + 3\|x - y\|^2 + 3\|y - x_{k'}\|^2 \\
&\leq 3\text{diam}(V_k) + 3\text{diam}(V_{k'}) + 3\|x - y\|^2 \\
&\leq 6 \max_k \text{diam}(V_k) + 3\|x - y\|^2,
\end{aligned} \tag{35}$$

where the first inequality is due to the fact that α_k^{ij} and $\beta_{k'}^{ij}$ are Kantorovich potentials of $W_2(\bar{\nu}_K^{(i)}, \bar{\nu}_K^{(j)})$ in (32). The second inequality comes from (30) where $\lambda = 1$. Defining the new cost function $c(x, y) = 6 \max_k \text{diam}(V_k) + 3\|x - y\|^2$, we thus define

$$\begin{aligned}
\text{OT}_c(\mu^{(i)}, \mu^{(j)}) &= 6 \max_k \text{diam}(V_k) + 3 \min_{\pi \in \Pi(\mu^{(i)}, \mu^{(j)})} \int \|x - y\|^2 d\pi(x, y) \\
&= 6 \max_k \text{diam}(V_k) + 3 W_2^2(\mu^{(i)}, \mu^{(j)}).
\end{aligned}$$

Now, by inequality (35), it follows that f^{ij} and g^{ij} are feasible Kantorovich potentials of OT_c between $\mu^{(i)}$ and $\mu^{(j)}$ in (34). Hence, we finally obtain from (33) that

$$\begin{aligned} W_2^2(\bar{\nu}_K^{(i)}, \bar{\nu}_K^{(j)}) &\leq \int_{\mathbb{R}^d} f^{ij}(x) d\mu^{(i)}(x) + \int_{\mathbb{R}^d} g^{ij}(y) d\mu^{(j)}(y) \\ &\leq \sup_{f,g: f(x)+g(y)\leq c(x,y)} \int_{\mathbb{R}^d} f(x) d\mu^{(i)}(x) + \int_{\mathbb{R}^d} g(y) d\mu^{(j)}(y) \\ &= 6 \max_k \text{diam}(V_k) + 3W_2^2(\mu^{(i)}, \mu^{(j)}), \end{aligned}$$

which concludes the proof. \square

Proof of Lemma 3.12. Suppose that the support of the mean measure $\bar{\mu}$ is included in $[0, 1]^d$. Then, we first have that $\max_{1 \leq k \leq K} \text{diam}(V_k) \leq \max_{1 \leq j \leq \lfloor \sqrt[d]{K} \rfloor^d} \text{diam}(V_j)$. Indeed, as $\lfloor \sqrt[d]{K} \rfloor^d \leq K$, this is simply reducing the number of quantization points, and therefore increasing the maximum diameter of the cells. Now, denoting $K' = \lfloor \sqrt[d]{K} \rfloor^d$ the d -th power of the integer $\lfloor \sqrt[d]{K} \rfloor$, one can grid the support space $[0, 1]^d$ with K' points $\{x_1, \dots, x_{K'}\}$ set as $\left\{ \left(\frac{a_1^{(i)}}{\lfloor \sqrt[d]{K} \rfloor}, \dots, \frac{a_d^{(i)}}{\lfloor \sqrt[d]{K} \rfloor} \right) \mid a_k^{(i)} \in \{1, \dots, d\} \right\}$. With these centers, all Voronoï cells have the same diameter, which is:

$$\forall 1 \leq k \leq K, \text{diam}(V_k) = \left\| \left(\frac{1}{\lfloor \sqrt[d]{K} \rfloor}, \dots, \frac{1}{\lfloor \sqrt[d]{K} \rfloor} \right) \right\|^2 = \sum_{i=1}^d \left(\frac{1}{\lfloor \sqrt[d]{K} \rfloor} \right)^2 = \frac{d}{\lfloor \sqrt[d]{K} \rfloor^2}.$$

This finally gives us:

$$\max_{1 \leq k \leq K} \text{diam}(V_k) \leq \frac{d}{\lfloor \sqrt[d]{K} \rfloor^2}.$$

\square

Proof of Proposition 3.13. For the result regarding the within-class variance of the clusters, we have, using the triangle inequality and (30) with $\lambda = 1$,

$$W_2^2(\nu_K^{(i)}, \nu_K^{(j)}) \leq 3(W_2^2(\nu_K^{(i)}, \mu^{(i)}) + W_2^2(\mu^{(i)}, \mu^{(j)}) + W_2^2(\mu^{(j)}, \nu_K^{(j)})) \quad (36)$$

Summing over the indices of I_l and dividing by N_l^2 yields:

$$\begin{aligned} \text{WCSS}(l, \nu_K) &\leq \frac{3}{N_l^2} \sum_{i,j \in I_l} W_2^2(\nu_K^{(i)}, \mu^{(i)}) + \frac{3}{N_l^2} \sum_{i,j \in I_l} W_2^2(\mu^{(i)}, \mu^{(j)}) + \frac{3}{N_l^2} \sum_{i,j \in I_l} W_2^2(\mu^{(j)}, \nu_K^{(j)}) \\ &\leq \frac{6}{N_l} \sum_{i \in I_l} W_2^2(\nu_K^{(i)}, \mu^{(i)}) + 3\text{WCSS}(l, \mu) \\ &\leq \frac{6}{N_l} \sum_{1 \leq i \leq N} W_2^2(\nu_K^{(i)}, \mu^{(i)}) + 3\text{WCSS}(l, \mu) = \frac{6N}{N_l} \varepsilon_K + 3\text{WCSS}(l, \mu), \end{aligned}$$

where the last equality follows from Proposition 3.4, which concludes the first item (19) of the proposition. For the second statement on the between-class variance, we rewrite the triangle inequality:

$$\begin{aligned} & 3(W_2^2(\nu_K^{(i)}, \mu^{(i)}) + W_2^2(\nu_K^{(i)}, \nu_K^{(j)}) + W_2^2(\mu^{(j)}, \nu_K^{(j)})) \geq W_2^2(\mu^{(i)}, \mu^{(j)}) \\ \Leftrightarrow & W_2^2(\nu_K^{(i)}, \nu_K^{(j)}) \geq \frac{1}{3}W_2^2(\mu^{(i)}, \mu^{(j)}) - W_2^2(\nu_K^{(i)}, \mu^{(i)}) - W_2^2(\mu^{(j)}, \nu_K^{(j)}) \end{aligned}$$

Summing over the indices of I_{l_1} and I_{l_2} and dividing by $N_{l_1}N_{l_2}$ gives:

$$\begin{aligned} \text{BCSS}(l_1, l_2, \nu_K) & \geq \frac{1}{3} \frac{1}{N_{l_1}N_{l_2}} \sum_{\substack{i_1 \in I_{l_1} \\ i_2 \in I_{l_2}}} W_2^2(\mu^{(i_1)}, \mu^{(i_2)}) \\ & \quad - \frac{1}{N_{l_1}N_{l_2}} \sum_{\substack{i_1 \in I_{l_1} \\ i_2 \in I_{l_2}}} W_2^2(\nu_K^{(i_1)}, \mu^{(i_1)}) - \frac{1}{N_{l_1}N_{l_2}} \sum_{\substack{i_1 \in I_{l_1} \\ i_2 \in I_{l_2}}} W_2^2(\mu^{(i_2)}, \nu_K^{(i_2)}) \\ & \geq \frac{1}{3} \text{BCSS}(l_1, l_2, \mu) - \frac{1}{N_{l_1}N_{l_2}} \sum_{1 \leq i_1, i_2 \leq N} W_2^2(\nu_K^{(i_1)}, \mu^{(i_1)}) \\ & \quad - \frac{1}{N_{l_1}N_{l_2}} \sum_{1 \leq i_1, i_2 \leq N} W_2^2(\nu_K^{(i_2)}, \mu^{(i_2)}) \\ & = \frac{1}{3} \text{BCSS}(l_1, l_2, \mu) - \frac{1}{N_{l_1}} \sum_{1 \leq i_1 \leq N} W_2^2(\nu_K^{(i_1)}, \mu^{(i_1)}) \\ & \quad - \frac{1}{N_{l_2}} \sum_{1 \leq i_2 \leq N} W_2^2(\nu_K^{(i_2)}, \mu^{(i_2)}) \\ & = \frac{1}{3} \text{BCSS}(l_1, l_2, \mu) - \left(\frac{1}{N_{l_1}} + \frac{1}{N_{l_2}} \right) \sum_{1 \leq i \leq N} W_2^2(\nu_K^{(i)}, \mu^{(i)}) \\ & = \frac{1}{3} \text{BCSS}(l_1, l_2, \mu) - \left(\frac{N}{N_{l_1}} + \frac{N}{N_{l_2}} \right) \varepsilon_K, \end{aligned}$$

where the last equality follows from Proposition 3.4, which concludes the proof. \square

The proof of Proposition 3.14 relies on the following Lemma which holds for any embedding ϕ .

Lemma A.2. *Let $\phi : \mathcal{P}(\mathcal{X}) \rightarrow \mathcal{H}$ be an embedding of probability measures (supported on an arbitrary set included in $\mathcal{X} \subset \mathbb{R}^d$) into a Hilbert space \mathcal{H} equipped with the inner-product $\langle \cdot, \cdot \rangle_{\mathcal{H}}$ and the induced norm $\|\cdot\|_{\mathcal{H}}$. Suppose that $\|\phi\|_{\infty} = \sup_{\mu \in \mathcal{P}(\mathcal{X})} \|\phi(\mu)\|_{\mathcal{H}} < \infty$. Then, we have that:*

$$\|G_{\mu}^{\phi} - G_{\nu_K}^{\phi}\|_F^2 \leq C \sum_{i=1}^N \|\phi(\mu^{(i)}) - \phi(\nu_K^{(i)})\|_{\mathcal{H}}^2 \quad (37)$$

where C is a constant depending on N and $\|\phi\|_{\infty}$.

Proof of Lemma A.2. First, let us write the Frobenius matrix norm of $G_\mu^\phi - G_{\nu_K}^\phi$:

$$\|G_\mu^\phi - G_{\nu_K}^\phi\|_F^2 = \sum_{i,j=1}^N |(G_\mu^\phi - G_{\nu_K}^\phi)_{ij}|^2 = \sum_{i,j=1}^N |\langle \phi(\mu^{(i)}), \phi(\mu^{(j)}) \rangle_{\mathcal{H}} - \langle \phi(\nu_K^{(i)}), \phi(\nu_K^{(j)}) \rangle_{\mathcal{H}}|^2 \quad (38)$$

Additionally, we have that:

$$\begin{aligned} \langle \phi(\mu^{(i)}), \phi(\mu^{(j)}) \rangle_{\mathcal{H}} - \langle \phi(\nu_K^{(i)}), \phi(\nu_K^{(j)}) \rangle_{\mathcal{H}} &= \langle \phi(\mu^{(i)}) - \phi(\nu_K^{(i)}), \phi(\mu^{(j)}) \rangle_{\mathcal{H}} + \langle \phi(\nu_K^{(i)}), \phi(\mu^{(j)}) \rangle_{\mathcal{H}} \\ &\quad - \langle \phi(\nu_K^{(i)}), \phi(\nu_K^{(j)}) \rangle_{\mathcal{H}} \\ &= \langle \phi(\mu^{(i)}) - \phi(\nu_K^{(i)}), \phi(\mu^{(j)}) - \phi(\nu_K^{(j)}) \rangle_{\mathcal{H}} + \langle \phi(\mu^{(i)}) - \phi(\nu_K^{(i)}), \phi(\nu_K^{(j)}) \rangle_{\mathcal{H}} \\ &\quad + \langle \phi(\nu_K^{(i)}), \phi(\mu^{(j)}) \rangle_{\mathcal{H}} - \langle \phi(\nu_K^{(i)}), \phi(\nu_K^{(j)}) \rangle_{\mathcal{H}} \\ &= \langle \phi(\mu^{(i)}) - \phi(\nu_K^{(i)}), \phi(\mu^{(j)}) - \phi(\nu_K^{(j)}) \rangle_{\mathcal{H}} + \langle \phi(\mu^{(i)}) - \phi(\nu_K^{(i)}), \phi(\nu_K^{(j)}) \rangle_{\mathcal{H}} \\ &\quad + \langle \phi(\mu^{(j)}) - \phi(\nu_K^{(j)}), \phi(\nu_K^{(i)}) \rangle_{\mathcal{H}}. \end{aligned}$$

Injecting this equality in (38) yields:

$$\begin{aligned}
\|G_\mu^\phi - G_{\nu_K}^\phi\|_F^2 &= \sum_{i,j=1}^N \left| \langle \phi(\mu^{(i)}) - \phi(\nu_K^{(i)}), \phi(\mu^{(j)}) - \phi(\nu_K^{(j)}) \rangle_{\mathcal{H}} + \langle \phi(\mu^{(i)}) - \phi(\nu_K^{(i)}), \phi(\nu_K^{(j)}) \rangle_{\mathcal{H}} \right. \\
&\quad \left. + \langle \phi(\mu^{(j)}) - \phi(\nu_K^{(j)}), \phi(\nu_K^{(i)}) \rangle_{\mathcal{H}} \right|^2 \\
&\leq 3 \sum_{i,j=1}^N \left| \langle \phi(\mu^{(i)}) - \phi(\nu_K^{(i)}), \phi(\mu^{(j)}) - \phi(\nu_K^{(j)}) \rangle_{\mathcal{H}} \right|^2 \\
&\quad + 3 \sum_{i,j=1}^N \left| \langle \phi(\mu^{(i)}) - \phi(\nu_K^{(i)}), \phi(\nu_K^{(j)}) \rangle_{\mathcal{H}} \right|^2 \\
&\quad + 3 \sum_{i,j=1}^N \left| \langle \phi(\mu^{(j)}) - \phi(\nu_K^{(j)}), \phi(\nu_K^{(i)}) \rangle_{\mathcal{H}} \right|^2 \\
&\leq 3 \sum_{i,j=1}^N \left\| \phi(\mu^{(i)}) - \phi(\nu_K^{(i)}) \right\|_{\mathcal{H}}^2 \left\| \phi(\mu^{(j)}) - \phi(\nu_K^{(j)}) \right\|_{\mathcal{H}}^2 \\
&\quad + 3 \sum_{i,j=1}^N \left\| \phi(\mu^{(i)}) - \phi(\nu_K^{(i)}) \right\|_{\mathcal{H}}^2 \left\| \phi(\nu_K^{(j)}) \right\|_{\mathcal{H}}^2 \\
&\quad + \sum_{i,j=1}^N \left\| \phi(\mu^{(j)}) - \phi(\nu_K^{(j)}) \right\|_{\mathcal{H}}^2 \left\| \phi(\nu_K^{(i)}) \right\|_{\mathcal{H}}^2 \\
&= 3 \left(\sum_{i=1}^N \left\| \phi(\mu^{(i)}) - \phi(\nu_K^{(i)}) \right\|_{\mathcal{H}}^2 \right)^2 + 6 \sum_{i,j=1}^N \left\| \phi(\mu^{(i)}) - \phi(\nu_K^{(i)}) \right\|_{\mathcal{H}}^2 \left\| \phi(\nu_K^{(j)}) \right\|_{\mathcal{H}}^2 \\
&\leq \sum_{i=1}^N \left\| \phi(\mu^{(i)}) - \phi(\nu_K^{(i)}) \right\|_{\mathcal{H}}^2 \left(3 \sum_{i=1}^N \left\| \phi(\mu^{(i)}) - \phi(\nu_K^{(i)}) \right\|_{\mathcal{H}}^2 + 6 \sum_{j=1}^N \left\| \phi(\nu_K^{(j)}) \right\|_{\mathcal{H}}^2 \right)
\end{aligned} \tag{39}$$

where (39) is due to Cauchy-Schwarz. By hypothesis, we have $\|\phi\|_\infty = \sup_{\mu \in \mathcal{P}(\mathcal{X})} \|\phi(\mu)\|_{\mathcal{H}} = M_\phi < \infty$. Therefore, (40) yields:

$$\begin{aligned}
\|G_\mu^\phi - G_{\nu_K}^\phi\|_F^2 &\leq \sum_{i=1}^N \left\| \phi(\mu^{(i)}) - \phi(\nu_K^{(i)}) \right\|_{\mathcal{H}}^2 \left(3 \sum_{i=1}^N M_\phi^2 + 6 \sum_{j=1}^N M_\phi^2 \right) \\
&= 9N M_\phi^2 \sum_{i=1}^N \left\| \phi(\mu^{(i)}) - \phi(\nu_K^{(i)}) \right\|_{\mathcal{H}}^2.
\end{aligned}$$

Choosing $C := 9N M_\phi^2$ concludes the proof. \square

Proof of Proposition 3.14. (ii) We first prove inequality (22) for the KME embedding $\phi : \sigma \in \mathcal{P}(\mathcal{X}) \mapsto \int k(x, \cdot) d\sigma(x) \in \mathcal{H}$. By hypothesis, the kernel k is bounded by a constant M_k . Therefore for any $\mu \in \mathcal{P}(\mathcal{X})$, we have $\|\phi(\mu)\|_{\mathcal{H}}^2 = \langle \int k(x, \cdot) d\mu(x), \int k(y, \cdot) d\mu(y) \rangle_{\mathcal{H}} = \iint k(x, y) d\mu(x) d\mu(y) \leq M_k$. By Lemma A.2, we then have

$$\|G_{\mu}^{\phi} - G_{\nu_K}^{\phi}\|_F^2 \leq C_{N,k} \sum_{i=1}^N \|\phi(\mu^{(i)}) - \phi(\nu_K^{(i)})\|_{\mathcal{H}}^2$$

with $C_{N,k} := 9NM_k$. Using the property $\text{MMD} \leq W_1 \leq W_2$, we obtain that

$$\begin{aligned} \frac{1}{N} \|G_{\mu}^{\text{KME}} - G_{\nu_K}^{\text{KME}}\|_F^2 &\leq \frac{C_{N,k}}{N} \sum_{i=1}^N \|\phi(\mu^{(i)}) - \phi(\nu_K^{(i)})\|_{\mathcal{H}}^2 = \frac{C_{N,k}}{N} \sum_{i=1}^N \text{MMD}^2(\mu^{(i)}, \nu_K^{(i)}) \\ &\leq \frac{C_{N,k}}{N} \sum_{i=1}^N W_2^2(\mu^{(i)}, \nu_K^{(i)}) \\ &= C_{N,k} \varepsilon_K. \end{aligned}$$

(i) In order to prove inequality (21) for the LOT embedding $\phi : \mu \in \mathcal{P}(\mathcal{X}) \mapsto T_{\rho}^{\mu} - \text{id} \in L^2(\rho)$ with a.c. reference measure ρ , we first note that for any measure $\mu \in \mathcal{P}(\mathcal{X})$, $\|\phi(\mu)\|_{L^2(\rho)}^2 = \int |T_{\rho}^{\mu}(x) - x|^2 d\rho(x) \leq \int \text{diam}(\mathcal{X})^2 d\rho(x) = \text{diam}(\mathcal{X})^2$. Then we can apply Lemma A.2 with constant $C := C_{N,\mathcal{X}} = 9N\text{diam}(\mathcal{X})^2$ in (37) and finally obtain

$$\frac{1}{N} \|G_{\mu}^{\text{LOT}} - G_{\nu_K}^{\text{LOT}}\|_F^2 \leq \frac{C_{N,\mathcal{X}}}{N} \sum_{i=1}^N \|T_{\rho}^{\mu^{(i)}} - T_{\rho}^{\nu_K^{(i)}}\|_{L^2(\rho)}^2. \quad (41)$$

We now use a result due to Ambrosio and reported in [17] and [14][Theorem (Ambrosio)], which states that when ρ is a probability density over a compact set \mathcal{X} , μ and ν are probability measures on a \mathcal{X} and T_{ρ}^{μ} is L -Lipschitz (by hypothesis), then:

$$\|T_{\rho}^{\mu} - T_{\rho}^{\nu}\|_{L^2(\rho)} \leq 2\sqrt{\text{diam}(\mathcal{X})L}W_1(\mu, \nu)^{1/2}. \quad (42)$$

Finally, assembling the inequalities (41) and (42), we obtain

$$\begin{aligned}
\frac{1}{N} \|G_\mu^{\text{LOT}} - G_{\nu_K}^{\text{LOT}}\|_F^2 &\leq \frac{C_{N,\mathcal{X}}}{N} \sum_{i=1}^N 4\text{diam}(\mathcal{X}) L W_1(\mu^{(i)}, \nu_K^{(i)}) \\
&\leq 4C_{N,\mathcal{X}} \text{diam}(\mathcal{X}) L \frac{1}{N} \sum_{i=1}^N W_2(\mu^{(i)}, \nu_K^{(i)}) \\
&= 4C_{N,\mathcal{X}} \text{diam}(\mathcal{X}) L \frac{1}{N} \sqrt{\left(\sum_{i=1}^N W_2(\mu^{(i)}, \nu_K^{(i)}) \right)^2} \\
&\leq 4C_{N,\mathcal{X}} \text{diam}(\mathcal{X}) L \frac{1}{N} \sqrt{N \sum_{i=1}^N W_2^2(\mu^{(i)}, \nu_K^{(i)})} \\
&= 4C_{N,\mathcal{X}} \text{diam}(\mathcal{X}) L \frac{1}{N} \sqrt{N \cdot N \varepsilon_K(\bar{\mu})} \\
&= 4C_{N,\mathcal{X}} \text{diam}(\mathcal{X}) L \cdot \sqrt{\varepsilon_K(\bar{\mu})} \\
&= C_{N,\mathcal{X},L} \sqrt{\varepsilon_K(\bar{\mu})},
\end{aligned}$$

which concludes the proof. \square

B Link between the diagonalization of the covariance operator and the Gram matrix of inner-products

In this section, we show that diagonalizing the Gram matrix of inner-products is closely related to diagonalizing the covariance operator in a Hilbert space. Suppose we have elements f_1, \dots, f_N belonging to a separable Hilbert space \mathcal{H} , endowed with the inner-product $\langle \cdot, \cdot \rangle_{\mathcal{H}}$. The covariance operator Σ of the data is defined as:

$$\forall h \in \mathcal{H}, \quad \Sigma(h) = \frac{1}{N} \sum_{i=1}^n f_i \langle f_i, h \rangle_{\mathcal{H}}.$$

We recall that $h \in \mathcal{H}$ is an eigenvector of Σ associated to the eigenvalue $\lambda \in \mathbb{R}$ if

$$\Sigma(h) = \frac{1}{N} \sum_{i=1}^n f_i \langle f_i, h \rangle_{\mathcal{H}} = \lambda h \tag{43}$$

Dividing by λ in (43), one obtains:

$$h = \sum_{i=1}^N \frac{1}{N\lambda} f_i \langle f_i, h \rangle_{\mathcal{H}} = \sum_{i=1}^N a_i f_i, \tag{44}$$

where $a_i = \frac{1}{N\lambda} \langle f_i, h \rangle_{\mathcal{H}} \in \mathbb{R}$. Injecting (44) in (43) yields:

$$\sum_{i=1}^N f_i \langle f_i, \sum_{j=1}^N a_j f_j \rangle_{\mathcal{H}} = N\lambda \sum_{i=1}^N a_i f_i \tag{45}$$

Taking the inner-product of (45) in with f_l yields:

$$\begin{aligned}
& \langle f_l, \sum_{i=1}^N f_i \langle f_i, \sum_{j=1}^N a_j f_j \rangle_{\mathcal{H}} \rangle_{\mathcal{H}} = \langle f_l, N\lambda \sum_{i=1}^N a_i f_i \rangle_{\mathcal{H}} \\
\Leftrightarrow & \sum_{i=1}^N \langle f_l, f_i \sum_{j=1}^N a_j \langle f_i, f_j \rangle_{\mathcal{H}} \rangle_{\mathcal{H}} = N\lambda \sum_{i=1}^N \langle f_l, f_i \rangle_{\mathcal{H}} \\
\Leftrightarrow & \sum_{i,j=1}^N a_j \langle f_i, f_j \rangle_{\mathcal{H}} \langle f_l, f_i \rangle_{\mathcal{H}} = N\lambda \sum_{i=1}^N a_i \langle f_l, f_i \rangle_{\mathcal{H}}.
\end{aligned}$$

If we note K the $N \times N$ Gram matrix of inner-products, that is $G_{ij} = \langle f_i, f_j \rangle_{\mathcal{H}}$, and $a = (a_1, \dots, a_N)^T \in \mathbb{R}^N$, then we can rewrite the previous inequality with matrix notations:

$$K^2 a = N\lambda K a \quad (46)$$

and a can be found solving

$$K a = N\lambda a \quad (47)$$

or equivalently by the diagonalization of the Gram matrix K . From a , one can recover the eigenelement h with (44).

C Additional numerical experiments

C.1 Synthetic dataset : an explicit formulation for the pairwise inner-products in the Gram matrix

Proposition C.1. *Let ρ be an a.c. probability measure with compact support, defined for $X \sim \rho$ by $X = R \frac{Z}{\|Z\|}$, where $R \sim \text{Unif}([0, 1])$ and $Z \sim \mathcal{N}(0, I_d)$ are independent random variable. Let $(\mu^{(i)})_{i=1}^N$ be N distributions defined by*

$$\mu^{(i)} = (\Sigma_i^{1/2} \text{id} + b_i)_{\#} \rho,$$

where $\Sigma_i \in \mathbb{R}^{d \times d}$ is a positive semi-definite matrix and $b_i \in \mathbb{R}^d$.

(i) For the LOT embedding, we choose ρ as the reference measure, for which $\phi(\mu^{(i)}) = T_{\rho}^{\mu^{(i)}} - \text{id}$. Then one has $\forall 1 \leq i, j \leq N$,

$$\langle \phi(\mu^{(i)}), \phi(\mu^{(j)}) \rangle_{L^2(\rho)} = \langle b_i, b_j \rangle + \frac{1}{3d} \langle \Sigma_i^{1/2} - I_d, \Sigma_j^{1/2} - I_d \rangle_F.$$

(ii) For the KME, we consider the specific kernel $k : \mathbb{R}^d \times \mathbb{R}^d \rightarrow \mathbb{R}$ given by $k(x, y) = x^T y + (x^T y)^2$, for which $\phi(\mu^{(i)}) = \int k(x, \cdot) d\mu^{(i)}(x)$. Then one has $\forall 1 \leq i, j \leq N$,

$$\langle \phi(\mu^{(i)}), \phi(\mu^{(j)}) \rangle_{\mathcal{H}} = \langle b_i, b_j \rangle + \langle b_i, b_j \rangle^2 + \frac{1}{3d} \langle \Sigma_j, b_i b_i^T \rangle_F + \frac{1}{3d} \langle \Sigma_i, b_j b_j^T \rangle_F + \frac{1}{9d^2} \langle \Sigma_i, \Sigma_j \rangle_F.$$

Proof of Proposition C.1. First, we have $\mathbb{E}[X] = \mathbb{E}[R] \cdot \mathbb{E}\left[\frac{Z}{\|Z\|}\right] = \frac{1}{2} \cdot 0 = 0$. Then we also have that $\text{Cov}[X] = \mathbb{E}[XX^T] = \mathbb{E}[R^2] \cdot \mathbb{E}\left[\frac{ZZ^T}{\|Z\|^2}\right] = \frac{1}{3} \cdot \frac{1}{d} I_d$.

(i) For LOT, we have

$$\begin{aligned}\langle \phi(\mu^{(i)}), \phi(\mu^{(j)}) \rangle_{L^2(\rho)} &= \langle T_\rho^{\mu^{(i)}} - \text{id}, T_\rho^{\mu^{(j)}} - \text{id} \rangle_{L^2(\rho)} \\ &= \int \langle T_\rho^{\mu^{(i)}}(x) - x, T_\rho^{\mu^{(j)}}(x) - x \rangle d\rho(x).\end{aligned}$$

Moreover, the optimal transport map between ρ and $\mu^{(i)}$ is made explicit in (23). Note that it is optimal in the sense of (5) since $x \mapsto \Sigma_i^{1/2}x + b_i$ is the gradient of a convex function, and Brenier's theorem [9] allows to conclude. Then

$$\langle T_\rho^{\mu^{(i)}} - \text{id}, T_\rho^{\mu^{(j)}} - \text{id} \rangle_{L^2(\rho)} = \int \langle \Sigma_i^{1/2}x + b_i - x, \Sigma_j^{1/2}x + b_j - x \rangle d\rho(x).$$

Let us write $C_i = \Sigma_i^{1/2} - I_d$ for simplicity of notation, then since ρ is centered:

$$\begin{aligned}\langle T_\rho^{\mu^{(i)}} - \text{id}, T_\rho^{\mu^{(j)}} - \text{id} \rangle_{L^2(\rho)} &= \int \langle C_i x + b_i, C_j x + b_j \rangle d\rho(x) \\ &= \int (C_i x)^T C_j x d\rho(x) + \int b_i^T b_j d\rho(x) \\ &\quad + \int (C_i x)^T b_j d\rho(x) + \int (C_j x)^T b_i d\rho(x) \\ &= b_i^T b_j + \int x^T C_i C_j x d\rho(x).\end{aligned}$$

Finally, using that $\mathbb{E}[XX^T] = \frac{1}{3d}I_d$,

$$\begin{aligned}\int x^T C_i C_j x d\rho(x) &= \int \text{Tr}(x^T C_i C_j x) d\rho(x) \\ &= \text{Tr}\left(\int C_i C_j x x^T d\rho(x)\right) \\ &= \text{Tr}\left(C_i C_j \int x x^T d\rho(x)\right) \\ &= \text{Tr}\left(C_i C_j \frac{1}{3d} I_d\right) \\ &= \frac{1}{3d} \text{Tr}(C_i C_j).\end{aligned}$$

And we get

$$\langle T_\rho^{\mu^{(i)}} - \text{id}, T_\rho^{\mu^{(j)}} - \text{id} \rangle_{L^2(\rho)} = \langle b_i, b_j \rangle + \frac{1}{3d} \langle \Sigma_i^{1/2} - I_2, \Sigma_j^{1/2} - I_2 \rangle_F. \quad (48)$$

(ii) For the KME embedding,

$$\begin{aligned}
\langle \phi(\mu^{(i)}), \phi(\mu^{(j)}) \rangle_{\mathcal{H}} &= \left\langle \int k(x, \cdot) d\mu^{(i)}(x), \int k(y, \cdot) d\mu^{(j)}(y) \right\rangle_{\mathcal{H}} \\
&= \iint \langle k(x, \cdot), k(y, \cdot) \rangle_{\mathcal{H}} d\mu^{(i)}(x) d\mu^{(j)}(y) \\
&= \iint k(x, y) d\mu^{(i)}(x) d\mu^{(j)}(y) \\
&= \iint [x^T y + (x^T y)^2] d\mu^{(i)}(x) d\mu^{(j)}(y) \\
&= \iint [x^T y + x^T y y^T x] d\mu^{(i)}(x) d\mu^{(j)}(y) \\
&= b_i^T b_j + \iint x^T y y^T x d\mu^{(i)}(x) d\mu^{(j)}(y) \\
&= b_i^T b_j + \iint \text{Tr}(x^T y y^T x) d\mu^{(i)}(x) d\mu^{(j)}(y) \\
&= b_i^T b_j + \iint \text{Tr}(y y^T x x^T) d\mu^{(i)}(x) d\mu^{(j)}(y) \\
&= b_i^T b_j + \text{Tr} \left(\iint y y^T x x^T d\mu^{(i)}(x) d\mu^{(j)}(y) \right) \\
&= b_i^T b_j + \text{Tr} \left(\int y y^T d\mu^{(j)}(y) \int x x^T d\mu^{(i)}(x) \right)
\end{aligned}$$

Now, since $\mu^{(i)} = (\Sigma_i^{1/2} \text{id} + b_i) \# \rho$, we have that :

$$\begin{aligned}
\int x x^T d\mu^{(i)}(x) &= \int (\Sigma_i^{1/2} x + b_i) (\Sigma_i^{1/2} x + b_i)^T d\rho(x) \\
&= \int (\Sigma_i^{1/2} x x^T \Sigma_i^{1/2} + \Sigma_i^{1/2} x b_i^T + b_i x^T \Sigma_i^{1/2} + b_i b_i^T) d\rho(x) \\
&= \Sigma_i^{1/2} \int x x^T d\rho(x) \Sigma_i^{1/2} + b_i b_i^T \\
&= \frac{1}{3d} \Sigma_i + b_i b_i^T.
\end{aligned}$$

This gives :

$$\begin{aligned}
\langle \phi(\mu^{(i)}), \phi(\mu^{(j)}) \rangle_{\mathcal{H}} &= b_i^T b_j + \text{Tr} \left(\left(\frac{1}{3d} \Sigma_i + b_i b_i^T \right) \left(\frac{1}{3d} \Sigma_j + b_j b_j^T \right) \right) \\
&= b_i^T b_j + \text{Tr} \left(\frac{1}{9d^2} \Sigma_i \Sigma_j + \frac{1}{3d} \Sigma_i b_j b_j^T + \frac{1}{3d} \Sigma_j b_i b_i^T + b_i b_i^T b_j b_j^T \right) \\
&= \langle b_i, b_j \rangle + \langle b_i, b_j \rangle^2 + \frac{1}{3d} \langle \Sigma_j, b_i b_i^T \rangle_F + \frac{1}{3d} \langle \Sigma_i, b_j b_j^T \rangle_F + \frac{1}{9d^2} \langle \Sigma_i, \Sigma_j \rangle_F
\end{aligned}$$

□

Figure 4 depicts the first components of PCA after KME on both quantization steps. As for LOT embedding, we see that for K as small as 32, the PCA visualizations with the two quantization methods look highly similar to the true PCA.

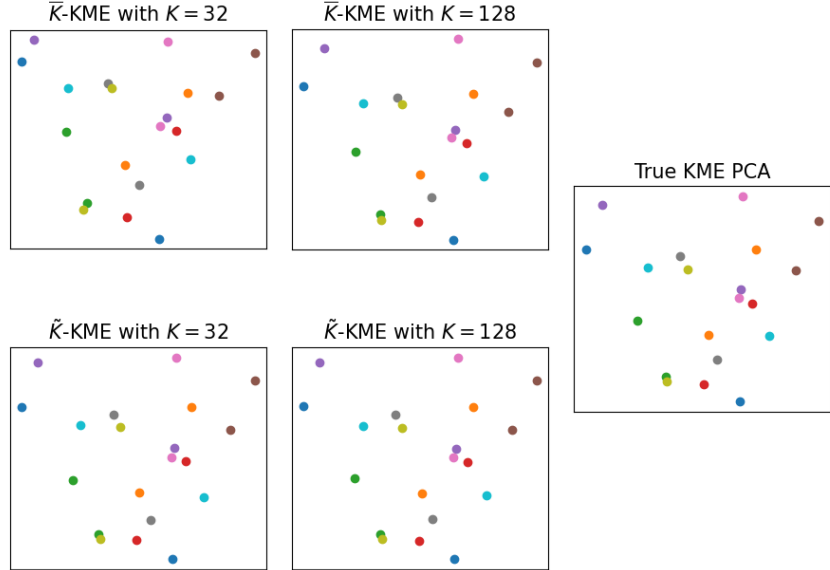


Figure 4: **Synthetic dataset on shifts and scalings.** Projection of the data onto the first two components of PCA after \bar{K} -KME (top) and \tilde{K} -KME (bottom) and comparison to the KME PCA (right) computed from the true Gram matrix (see Prop.C.1).

C.2 Visualization of the flow cytometry dataset

In this section, we show in Figures 5 and 6 the projections of the embedded data (by either K -LOT or K -KME) on the first components of PCA. We see that the first two components already allow to discriminate the flow cytometry measurements according to their labels.

C.3 Earth image dataset

We display in Figure 7 a few samples of the earth image dataset.

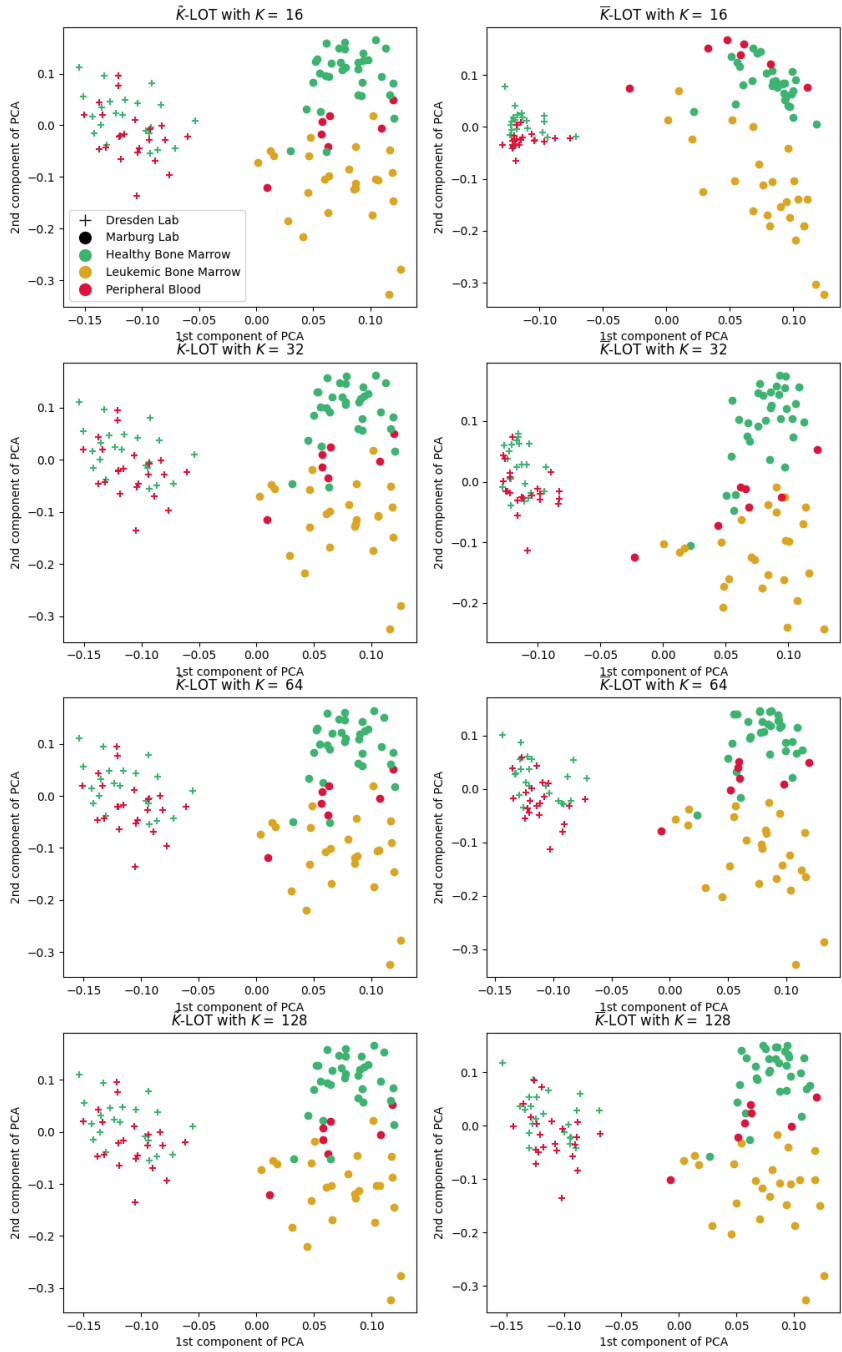


Figure 5: **Flow cytometry dataset.** Projection of the $N = 108$ measures on the first components of PCA after embedding with K -LOT.

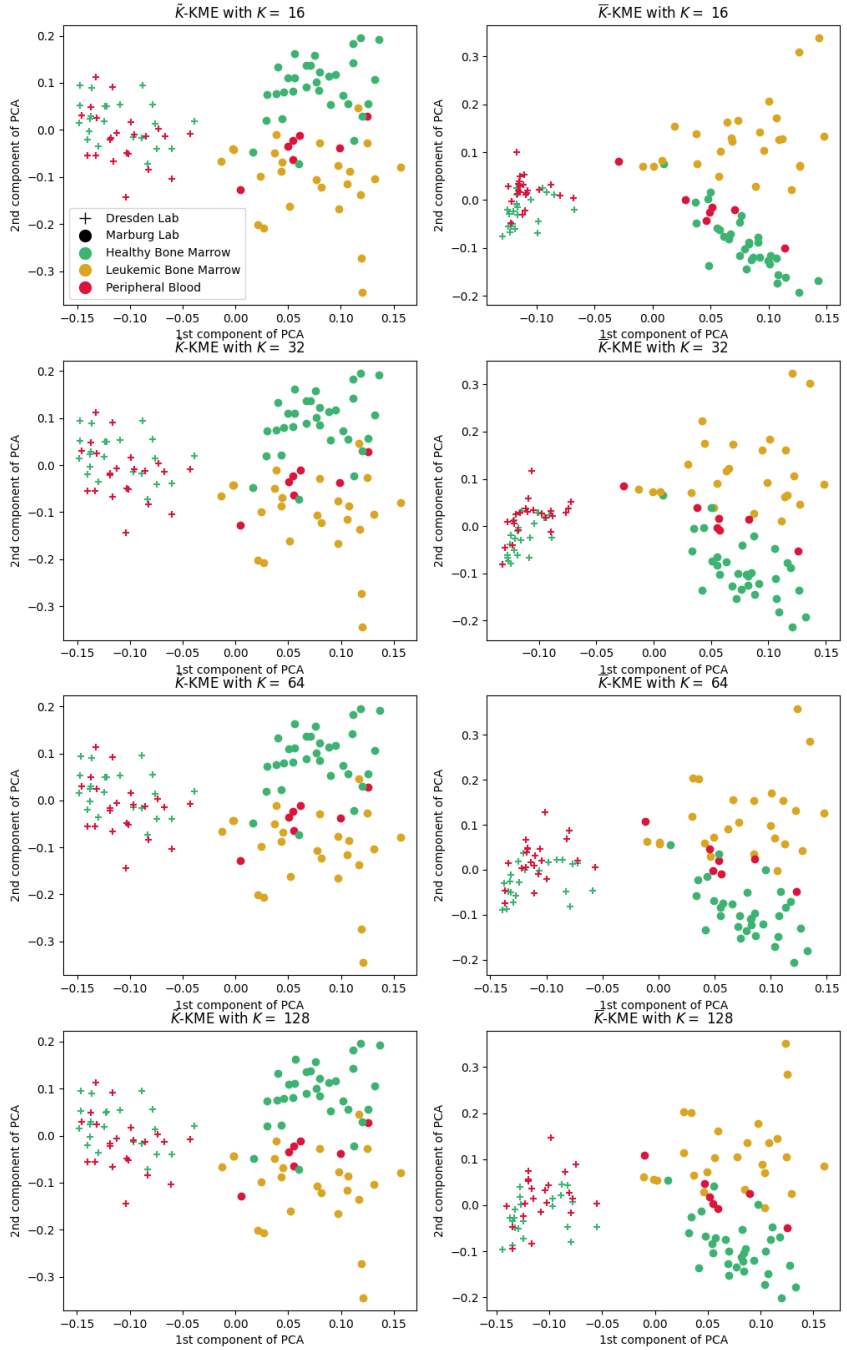


Figure 6: **Flow cytometry dataset.** Projection of the $N = 108$ measures on the first components of PCA after embedding with K -KME with RBF kernel with $\sigma = 1$.



(a) With wind turbine

(b) Without wind turbines

Figure 7: **Earth image dataset.** Examples of images sampled from the Airbus dataset.